Received Date: 29-Nov-2015

Revised Date: 11-Feb-2016

Accepted Date: 12-Feb-2016

Article Type: Articles

Stoichiometry of microbial carbon use efficiency in soils

ROBERT L. SINSABAUGH[1], BENJAMIN L. TURNER[2], JENNIFER M. TALBOT[3], BONNIE G. WARING[4], JENNIFER S. POWERS[5], CHERYL R. KUSKE[6], DARYL L. MOORHEAD[7], JENNIFER J. FOLLSTAD SHAH[8]

1 Department of Biology, University of New Mexico, Albuquerque, NM, 87131. rlsinsab@unm.edu.

2 Smithsonian Tropical Research Institute, Apartado 0843-03092, Balboa, Ancon, Republic of Panama. TurnerBL@si.edu

3 Department of Biology, Boston University, 5 Cummington Mall, Boston, MA, 02215, jmtalbot@bu.edu.

4 Department of Ecology and Evolution, University of Minnesota, St Paul, MN 55108, USA. bonnie.waring@gmail.com.

5 Departments of Ecology, Evolution and Behavior and Plant Biology, University of Minnesota, St. Paul, MN, 55108, USA. powers@umn.edu

This article has been accepted for publication and undergone full peer review but has not been through the copyediting, typesetting, pagination and proofreading process, which may lead to differences between this version and the Version of Record. Please cite this article as doi: 10.1890/15-2110.1
This article is protected by copyright. All rights reserved.

Accepted Article

6 Bioscience Division, Los Alamos National Laboratory, Los Alamos, NM, 87545, USA. kuske@lanl.gov

7 Department of Environmental Sciences, University of Toledo, 2810 W Bancroft St, Toledo, Ohio 43606, USA. daryl.moorhead@utoledo.edu

8 Environmental and Sustainable Studies Program, University of Utah, 260 S. Central Campus Drive, Salt Lake City, UT 84112, USA. jennifer.shah@envst.utah.edu

Abstract. The carbon use efficiency (CUE) of microbial communities partitions the flow of C from primary producers to the atmosphere, decomposer food webs and soil C stores. CUE, usually defined as the ratio of growth to assimilation, is a critical parameter in ecosystem models, but is seldom measured directly in soils because of the methodological difficulty of measuring *in situ* rates of microbial growth and respiration. Alternatively, CUE can be estimated indirectly from the elemental stoichiometry of organic matter and microbial biomass, and the ratios of C to nutrient-acquiring ecoenzymatic activities. We used this approach to estimate and compare microbial CUE in >2000 soils from a broad range of ecosystems. Mean CUE based on C:N stoichiometry was 0.269 ± 0.110 (SD). A parallel calculation based on C:P stoichiometry yielded a mean CUE estimate of 0.252 ± 0.125 (SD). The mean values and frequency distributions were similar to those from aquatic ecosystems, also calculated from stoichiometric models, and to those calculated from direct measurements of bacterial and fungal growth and respiration. CUE was directly related to microbial biomass C with a scaling exponent of 0.304 ± 0.067 (95% CI) and inversely related to microbial biomass P with a scaling exponent of -0.234 ± 0.055 (95% CI). Relative to CUE, biomass specific turnover time increased with a scaling

This article is protected by copyright. All rights reserved.

Accepted Article

exponent of 0.509 ± 0.042. CUE increased weakly with mean annual temperature. CUE declined with increasing soil pH reaching a minimum at pH 7.0, then increased again as soil pH approached 9.0, a pattern consistent with pH trends in the ratio of fungal:bacteria abundance and growth. Structural equation models that related geographic variables to CUE component variables showed the strongest connections for paths linking latitude and pH to ß-glucosidase activity and soil C:N:P ratios. The integration of stoichiometric and metabolic models provides a quantitative description of the functional organization of soil microbial communities that can improve the representation of CUE in microbial process and ecosystem simulation models.

Key words: carbon use efficiency, ecological stoichiometry, microbial communities, biomass turnover, ecoenzymatic activity

INTRODUCTION

The carbon use efficiency (CUE) of microorganisms partitions the flow of carbon (C) through terrestrial ecosystems, regulating atmospheric exchanges and soil C sequestration (Bradford et al. 2013, Clemmensen et al. 2013). Microbial CUE is a critical parameter in ecosystem models, but it is seldom measured directly because of the methodological difficulty of measuring *in situ* rates of microbial growth and respiration. Models commonly assume fixed values based on literature syntheses even though microbial CUE varies in response to available resources and biomass composition (Manzoni et al. 2012, Sinsabaugh et al. 2013, 2015). This assumption reduces the accuracy and utility of terrestrial ecosystem models that simulate soil C dynamics (Bradford and Crowther 2013, Lee and Schmidt 2014). At present, however, there are insufficient data to establish empirical relationships between CUE and its environmental correlates that might improve the representation of CUE in ecosystem simulation models.

This article is protected by copyright. All rights reserved.

Accepted Article

Accepted Article

For microorganisms, CUE is most commonly defined as the ratio of growth to assimilation, measured in units of C, with assimilation estimated as the sum of growth (μ) and respiration (R): CUE = $\mu/(\mu+R)$. In practice, there are multiple ways to estimate CUE. Microbial growth can be measured as rates of biomass increase, protein synthesis, DNA replication or consumption of ^{13}C-labeled substrates. Respiration can be measured as rates of total CO_2 efflux, $^{13}CO_2$ efflux from labeled substrates, oxygen consumption or respiratory electron transport. These methodological choices can lead to CUE estimates that vary by a factor of two or more. In general, broader measures of community growth (e.g. protein biosynthesis) and respiration (e.g. whole community CO_2 efflux) yield lower values of CUE than estimates based on the uptake and respiration of specific substrates (Manzoni et al. 2012, Sinsabaugh et al. 2013). This methodological contingency complicates comparisons across studies and ecosystems, particularly for terrestrial soils because it is difficult to measure microbial growth and respiration in a medium with discontinuous water availability in an environment where a substantial portion of the microbiota live in symbiotic association with plants (Manzoni et al. 2012, Sinsabaugh et al. 2013, Zechmeister-Boltenstern et al. 2015). As a consequence there are relatively few estimates of microbial CUE in soils and it is difficult to parse methodological and mechanistic contributions to CUE variance.

An alternative to direct measurements of microbial respiration and growth is to estimate CUE from ecological stoichiometry (Sterner and Elser 2002, Cherif and Loreau 2007). From this perspective, the CUE of an organism is a function of the difference between its elemental requirements for growth and the composition of environmental substrate. This relationship is most often expressed as

$$TER_{C:X} / B_{C:X} = A_X/CUE, \text{ or } CUE = (B_{C:X} \bullet A_X) / TER_{C:X} \quad [1]$$

This article is protected by copyright. All rights reserved.

where X usually represents N or P; $B_{C:X}$ is the elemental C:N or C:P ratio of biomass; A_X is the apparent assimilation efficiency for nitrogen (N) or phosphorus (P); and $TER_{C:X}$ is the threshold element ratio for C:N or C:P (Sterner and Elser 2002, Elser et al. 2003, Frost et al. 2006). For osmotrophic bacteria and fungi, apparent assimilation efficiency is defined as the ratio of microbial substrate consumption to extracellular substrate generation (Sinsabaugh and Follstad Shah 2012). The TER is defined as the element ratio corresponding to balanced microbial growth, i.e. neither C nor nutrient limited.

Sinsabaugh and Follstad Shah (2012) extended this model by proposing that the $TER_{C:X}$ $/B_{C:X}$ term, which is difficult to estimate directly, was proportional to the term $EEA_{C:X}$ / $(B_{C:X}/L_{C:X})$, where $EEA_{C:X}$ is the ratio of ecoenzymatic activities directed toward acquiring C and X from the environment and $L_{C:X}$ is elemental composition of the substrate consumed. In this formulation, CUE is a function of the capacity of microbial communities, through physiological adaptation and population selection, to alter enzyme expression and biomass composition to mitigate differences between environmental resources and growth requirements, with the goal of maximizing growth rate. An assumption of this approach is that indicator enzyme activities have steady state scaling coefficients of approximately 1.0 in relation to microbial production and organic matter concentration, which is supported by empirical data (Sinsabaugh et al. 2015). An additional assumption is that microbial communities exhibit optimum resource allocation with respect to enzyme expression and environmental resources (Allison and Vitousek 2005, Hernandez and Hobbie 2010, Burns et al. 2013). A meta-analysis of environmental enzyme activities (V) in relation to substrate availability (S) yielded a common steady state elasticity coefficient ($\varepsilon = \delta(\ln V) / \delta(\ln S)$) of approximately 0.5 for a wide variety of hydrolytic, oxidative, assimilatory and dissimilatory enzymes, indicating that enzyme expression is regulated at the

This article is protected by copyright. All rights reserved.

Accepted Article

transcription level to optimize responsiveness to fluctuations in substrate availability (Sinsabaugh et al. 2014).

From these relationships, CUE is calculated as:

$CUE_{C:X} = CUE_{max}[S_{C:X}/(S_{C:X} + K_X)]$, where $S_{C:X} = (1/EEA_{C:X})(B_{C:X} / L_{C:X})$. [2]

$S_{C:X}$ is a scalar that represents the extent to which the allocation of ecoenzymatic activities offsets the disparity between the elemental composition of available resources and the composition of microbial biomass. On that basis, the half-saturation constant K_X has a value of 0.5. CUE_{max} is the upper limit for microbial growth efficiency (0.6) based on thermodynamic constraints. This formulation is consistent with Michaelis-Menten kinetics and metabolic control analysis (Cornish-Bowden 2012). In terms of the latter, increasing the activity or concentration of an enzyme at the beginning of a pathway has progressively less effect on the flux through a pathway. For example, an increment in the abundance of extracellular enzymes that produce glucose will not proportionally increase glucose uptake or flux through the glycolysis pathway.

Using mean values for the parameters in eq. 2, the average CUE for microbial communities in terrestrial soils, freshwater sediments and planktonic environments was estimated as 0.29, 0.27 and 0.28, respectively (Sinsabaugh and Follstad Shah 2012). For comparison, a meta-analysis of bacterial and fungal CUE calculated from direct measurements of growth and respiration yielded mean CUE values of 0.336 ± 0.213 (SD) and 0.326 ± 0.196, respectively (Sinsabaugh et al. 2015). Because the distribution of these data has a negative skew the median values (0.281 and 0.296, respectively) more closely approximate the stoichiometric CUE estimates.

The principal advantages of estimating CUE from stoichiometric relationships are that (1) the component parameters can be readily measured; (2) the approach can be applied at high

This article is protected by copyright. All rights reserved.

Accepted Article

spatial and temporal resolution; and (3) the approach is phenomenological because CUE is calculated from variables known to influence CUE. Equation 2 provides a template for establishing empirical relationships between CUE, organic matter composition, microbial biomass composition, nutrient availabilities and microbial metabolism. These relationships, in turn, provide a foundation for improving the representation of microbial processes in ecosystem simulation models.

We systematically evaluated eq. 2 by assembling stoichiometric data from studies that included measurements of the elemental C:N and C:P composition of soil organic matter and microbial biomass, and the potential activities of ß-1,4-glucosidase, ß -1,4-N-acetylglucosaminidase, leucine (alanine) aminopeptidase and acid (alkaline) phosphatase, a total of 2046 cases representing approximately 200 sites that span a broad range of natural and managed ecosystems (Table 1). CUE values were calculated independently for C:N and C:P stoichiometries and compared with those reported from other studies.

The first step in our analyses was to examine the partial regressions between CUE and each of its component variables. The second stage compared the correlation between $CUE_{C:N}$ and $CUE_{C:P}$ and the dependence of that relationship on the elemental N:P ratios of biomass and substrate. Next we evaluated the theoretical relationship between CUE and threshold element ratio (TER) by comparing TER values predicted from eq. 1 to empirical relationships between CUE and elemental substrate composition. From there, we determined the scaling coefficients for CUE and microbial biomass, i.e. the increment in CUE per increment in biomass, which in turn defined the relationship between CUE and biomass turnover rate. Finally, we rearranged eq. 2 to predict microbial nutrient use efficiencies and compared the values to those reported in other studies. For each stage of analysis, we present empirical trends using partial regression models,

This article is protected by copyright. All rights reserved.

Accepted Article

highlight differences between ecosystems where comparisons were possible, and compare the results to other representations from the literature.

Collectively, these analyses provide a broad empirical evaluation of the relationships presented in equations 1 and 2 that can be applied to microbial process models. For larger scale comparisons, we used structural equation models to link CUE and its component parameters to master variables of mean annual temperature, mean annual precipitation and soil pH. These statistical models provide additional information for simulation models by resolving the relative strength of ecosystem variables on CUE variance.

METHODS

Data from published studies

We searched the literature for studies of terrestrial soil and litter that included, at a minimum, measurements of the potential activities of ß -1,4-glucosidase (BG) and ß -1,4-N-acetylglucosaminidase (NAG), and the elemental C and N content of organic matter. The search yielded a total of 66 published studies (Table S1). Most studies (39) also included data on the potential activity of leucine aminopeptidase (LAP), alanine aminopeptidase (AAP) or other enzymatic indicators of proteolytic potential. Only 24 studies included direct measurements of microbial biomass C and N content. Five studies included data on acid (alkaline) phosphatase activity (AP) and soil C:P ratio, and two studies included microbial biomass C:P ratio.

Data were extracted from tables and figures. In almost all cases, these values were presented as means from multiple samples collected from specific sites, treatments, horizons or dates. For studies in which we participated directly, we included full data sets when each sample had independent measurements of the CUE component variables. In cases where there was only a single estimate of organic matter C:N or C:P ratio for a site, treatment or date, but multiple

This article is protected by copyright. All rights reserved.

Accepted Article

EEA samplings, the EEA data were averaged to create a single case for inclusion in the meta-analyses.

For each study, we also collected information on mean annual temperature (MAT), mean annual precipitation (MAP), soil pH, soil taxonomy, latitude, longitude, elevation and ecosystem type (Table S1). Notes on sampling and methodology were also included. The total number of cases from published studies was 794.

Data from new studies

In addition to published studies, our meta-analysis also included previously unpublished data from the authors. The largest data set, 659 cases, comes from analyses of A horizons from 71 tropical forest sites in Panama conducted by Turner (Table S2). These cases include measurements of soil and microbial biomass C, N and P, as well as ß -1,4-glucosidase, ß -1,4-N-acetylglucosaminidase, and phosphatase. Analytical methods are described in Turner and Wright (2014).

Talbot et al. (2014) measured soil C and N and the activities of ß -1,4-glucosidase, ß -1,4-N-acetylglucosaminidase and leucine aminopeptidase for O and A horizon samples from 27 pine forest sites distributed across North America, yielding 511 cases (Table S3). Sampling strategy and analytical methods are described in Talbot et al. (2014).

Kuske et al. analyzed Oe, Oa and A horizon samples collected from the Duke Forest FACE site (North Carolina, USA) in October 2012 for soil C and N and the activities of ß -1,4-glucosidase, ß -1,4-N-acetylglucosaminidase and alanine aminopeptidase, yielding 36 cases divided between ambient and N amended plots within rings 1, 5 and 6 (Table S4). Analytical methods follow those presented by Finzi et al. (2006).

Accepted Article

This article is protected by copyright. All rights reserved.

Waring et al. (2015) analyzed A horizon soils collected in October 2013 from three tropical dry forests in Costa Rica for soil and microbial biomass C, N and P and ß -1,4-glucosidase, ß -1,4-N-acetylglucosaminidase, leucine aminopeptidase and phosphatase activities, yielding 42 cases (Table S4). Sampling strategy and analytical methods are presented by Waring et al. (2015). Metadata on latitude, longitude, MAT, MAP, altitude and soil pH are also included in Tables S2- S4.

Carbon use efficiency calculation

Microbial CUE was calculated using eq. 2. EEA values were converted to units of nmol per g dry mass per h, or nmol per g organic matter (OM) per h, in cases where OM concentrations per g dry mass were not provided. $EEA_{C:N}$ was calculated as BG/(NAG+PEP), where PEP represents leucine or alanine aminopeptidase (LAP or AAP), or in a small number of cases other measures of proteolytic activity (Table S1). For studies involving acidic soils or litter that did not include measures of proteolytic potential, we estimated LAP from a linear regression model, using data from similar studies ($\ln LAP = 0.65 \bullet \ln BG - 0.43$, $R^2=0.41$, n=192). Peptidase activities in acidic soils were generally low, averaging 10.7% of BG and 11.6% of NAG, so the impact of these estimates on $EEA_{C:N}$ is relatively small. However, filling these gaps allows $EEA_{C:N}$ estimates from these studies to be directly compared to those from alkaline soil and aquatic environments, where LAP activity is often comparable to BG in magnitude, and both activities are much greater than NAG (Sinsabaugh and Follstad Shah 2012).

Molar ratios of soil organic C: total N (SOC:TN) were used as estimates of $L_{C:N}$. Microbial biomass C:N was also calculated as molar ratios. For studies that lacked direct estimates of microbial biomass C and N (Tables S1-S4), we used a mean molar $B_{C:N}$ ratio of 8.6 based on the meta-analysis by Cleveland and Liptzin (2007).

This article is protected by copyright. All rights reserved.

Five published studies plus the tropical ecosystem studies by Turner (Table S2) and Waring et al. (2015) included data for calculating microbial CUE from both C:P and C:N stoichiometry (n=694). For these cases, $EEA_{C:P}$ was calculated as the ratio of ß -1,4-glucosidase: acid (alkaline) phosphatase activity (BG/AP). $L_{C:P}$ was calculated as the molar ratio of soil organic C: soil organic P. Total P was used when SOP was not available (about 30 cases), which increases the corresponding $CUE_{C:P}$ estimates. Three of the published studies lacked direct measurements of microbial biomass C and P. For those cases (n=37), we used a mean molar $B_{C:P}$ ratio of 60 (Cleveland and Liptzin 2007) in the CUE calculations.

The data and resulting CUE calculations were also used to estimate values for two other parameters that appear in equation 1: apparent assimilation efficiencies for N and P (A_N and A_P) and the threshold element ratios (TER) for C:N and C:P. For our data, A_N and A_P estimates were calculated as:

$$A_X = CUE_{C:X} / S_{C:X} = [CUE_{C:X} / B_{C:X}] \bullet L_{C:X} \bullet EEA_{C:X} \qquad [3]$$

The threshold element ratios (TER) for C:N and C:P were calculated as:

$$TER_{C:X} = [A_X \bullet B_{C:X}] / CUE_{C:X} = L_{C:X} \bullet EEA_{C:X} \qquad [4]$$

Statistical analysis

Partial regressions were used to examine the relationships between CUE and its component and cognate variables (StatPlus ver. 5.9.5). The regressions highlight the relative strength and residual distributions of various associations based on observed data. These relationships are intrinsically autocorrelated through equations 1 and 2; no causality is assumed. The intent was to identify ecological trends and provide empirical relationships for process models.

This article is protected by copyright. All rights reserved.

Accepted Article

At larger scale, the relationships between CUE, its components and geographic variables were investigated using recursive structural equation models (SEM, Ωnyx, ver. 1.06). Our *a priori* C:N model included four observed exogenous variables (latitude, MAT, MAP, and soil pH) and five observed endogenous variables (BG, NAG+LAP, $L_{C:N}$, $B_{C:N}$, $CUE_{C:N}$). All variables were standardized using z-transformation to homogenize the variances. There were fixed covariance paths among each exogenous variable, and each exogenous variable was connected to each $CUE_{C:N}$ component variable by a free directional pathway. The four $CUE_{C:N}$ component variables were interconnected by fixed covariance paths (disturbance correlations) and each of the four variables was linked to $CUE_{C:N}$ by a free directional path. The fixed covariance values were taken from a covariance matrix generated for the entire data set (n=1827, litter bag studies were excluded from the SEM). The same *a priori* design was used for the C:P model, substituting AP, $L_{C:P}$ and $B_{C:P}$ and using covariance values specific to the data set. The *a priori* models were used to diagram the relative strength of the directional connections among variables. Nested *post hoc* models were created by progressively deleting weak connections between exogenous and endogenous variables until a likelihood ratio threshold of p=0.05 was approached.

RESULTS

Carbon use efficiency and ecological stoichiometry

For the data set as a whole (n=2046), the arithmetic mean $L_{C:N}$, $B_{C:N}$ and $EEA_{C:N}$ ratios were 22.2 ± 14.9 (SD), 7.91 ± 2.42 and 1.316 ± 1.214, respectively (Table 2). The $CUE_{C:N}$ estimates were normally distributed with an arithmetic mean of 0.269 ± 0.110 (Table 2, Fig. 1). The arithmetic means for A_N and $TER_{C:N}$ were 0.658 ± 0.213 and 28.8 ± 34.9, respectively (Table 2). For the subset of wet tropical forest sites (Turner, Table S2), the arithmetic means were $L_{C:N}$ 13.8 ± 2.1, $B_{C:N}$ 5.97 ± 1.54, $EEA_{C:N}$ 1.095 ± 0.478 and $CUE_{C:N}$ 0.278 ± 0.077. For

This article is protected by copyright. All rights reserved.

the subset of North American conifer sites (Talbot et al., Table S3), the arithmetic means were $L_{C:N}$ 30.5 ± 12.2, $EEA_{C:N}$ 1.422 ± 1.017 and $CUE_{C:N}$ 0.218 ± 0.096.

For studies that included data on C:P stoichiometry (n=713), the arithmetic mean $L_{C:P}$ and $B_{C:P}$ ratios were 1211 ± 1074 (SD) and 42.2 ± 49.6, respectively (Table 2). The arithmetic mean $EEA_{C:P}$ ratio was 0.180 ± 0.198, indicating strong P limitation. The arithmetic mean $CUE_{C:P}$ was 0.252 ± 0.125. The $CUE_{C:P}$ distribution showed a slight positive skew (0.08) with a median value of 0.242 (Table 2, Fig. 1). The arithmetic means for A_P and $TER_{C:P}$ were 0.687 ± 0.240 and 138 ± 235, respectively (Table 2).

Among its component variables, $CUE_{C:N}$ was most closely associated with $EEA_{C:N}$ and $L_{C:N}$. Excluding cases that lacked direct measures of peptidase activity, $CUE_{C:N}$ declined as $EEA_{C:N}$ (R^2 = 0.79, Fig. 2a) and $L_{C:N}$ (R^2 = 0.23, Fig. 2b) increased. Excluding cases that lacked direct measures of biomass C and N, $CUE_{C:N}$ increased with $B_{C:N}$ (R^2 = 0.20, Fig. 2c) and $B_{C:N}$ / $L_{C:N}$ (R^2 = 0.24, Fig. 2d). The regression model [$CUE_{C:N}$ = -0.09612•(ln $L_{C:N}$) – 0.12145•(ln $EEA_{C:N}$) + 0.5525] accounted for 88.5% of the variance in $CUE_{C:N}$ (F=7887, n=2046).

In contrast, $CUE_{C:P}$ was most closely associated with $B_{C:P}$ (R^2 = 0.60, Fig. 3c) and $EEA_{C:P}$ (R^2 = 0.38, Fig. 3a) and only weakly correlated with $L_{C:P}$ (R^2=0.01, Fig. 3b) and $B_{C:P}$ / $L_{C:P}$ (R^2=0.17, Fig. 3d). The poor relationship with $L_{C:P}$ and $CUE_{C:P}$ suggests that the SOC:SOP ratio was not a good indicator of P bioavailability. The regression model [$CUE_{C:P}$ = 0.1246•(ln $B_{C:P}$) – 0.0569•(ln $EEA_{C:P}$) – 0.3109] accounted for 73.2% of the variance in $CUE_{C:P}$ (F=945, n=694).

The CUE estimates calculated independently from C:N and C:P stoichiometry were weakly correlated (R^2 = 0.16, Fig 4a) because N:P ratios varied among samples. The regression slope (0.57 ± 0.10, 95% CI) was equal to the product of mean $EEA_{N:P}$ (0.105) and mean $B_{N:P}$

This article is protected by copyright. All rights reserved.

Accepted Article

(5.441) and the intercept was equal to $1/L_{N:P}$. The two values converge when normalized to $L_{N:P}$ ($R^2 = 0.79$, Fig. 4b).

The CUE estimates for C:N and C:P stoichiometry can also be linked through threshold element ratios (Fig. 5a,c). The two values were equal only when the ratio of $TER_{C:P}$ to $TER_{C:N}$ corresponded to the mean N:P ratio of microbial biomass ($B_{C:P}/B_{C:N} = 42.1/6.4 = 6.6$).

For the data set as a whole, the C:N ratio of soils often overlapped with the $TER_{C:N}$ with peak $CUE_{C:N}$ occurring at $L_{C:N}$ ratios somewhat greater than the estimated $TER_{C:N}$ ($L_{C:N} - TER_{C:N} \approx$ 10-30, Fig. 5b). But for tropical systems, the C:P ratios of organic matter were on average 10x greater than the $TER_{C:P}$. As a result, there was no trend between $[L_{C:P} - TER_{C:P}]$ and $CUE_{C:P}$ (Fig 5d), consistent with the weak relationship between $L_{C:P}$ and $CUE_{C:P}$ shown in Fig. 3b.

Sinsabaugh and Follstad Shah (2012) suggested that the square root of the product $CUE_{C:N} \bullet CUE_{C:P}$ might be a better estimate of microbial community CUE given the methodological problems intrinsic to measurements of microbial biomass composition and ecoenzymatic potential, and the tenuous connection between the bulk elemental composition of organic matter and the labile substrate consumption of microbial communities. This calculation yielded an average CUE of 0.255 ± 0.092 (SD, n=692) for our tropical data sets (Tables S2, S4). This composite CUE increased as microbial biomass C increased with a scaling coefficient (δ ln(CUE)/ δ ln(MBC)) of 0.302 ± 0.057 (95% CI, $R^2 = 0.144$, n=641, F=108, Fig. 6a). A parallel regression showed that CUE decreased as microbial biomass P increased with a scaling coefficient of -0.254 ± 0.042 (95% CI, $R^2 = 0.174$, n=653, F=137, Fig. 6b). The relationship between CUE and microbial biomass N was weak with a scaling coefficient of 0.069 ($R^2 = 0.01$, n=620, F = 4.3, p = 0.038) that was not significantly different from zero.

This article is protected by copyright. All rights reserved.

Accepted Article

Carbon use efficiency and fertilization

Our meta-analysis included data from agricultural sites as well as results from natural systems that were experimentally manipulated with nutrient additions. For the data set as a whole, the mean $CUE_{C:N}$ for fertilized soils (agricultural systems and experimental nutrient manipulations) did not differ from that of unfertilized soils (fertilized CUE 0.285, n=199, unfertilized CUE 0.278, n=183, F=0.50). Fertilization may have affected growth rates, but physiological adaptation and population selection appeared to stabilize $CUE_{C:N}$.

Carbon use efficiency and biomass turnover

Three studies included estimates of respiration rate per unit biomass (R/B also known as qCO_2). From these values, biomass turnover rate (μ/B) was calculated as $qCO_2 \bullet CUE_{C:N}/(1-CUE_{C:N})$, where CUE in this case was defined as μ/(μ+R). Biomass turnover time (T_B) decreased with increasing CUE (R^2=0.40) with a mean value of 58 d (Fig. 7a). Extrapolating this regression to the full data set yielded a mean microbial biomass turnover time of 67 ± 22 d (SD).

A more comprehensive approach to linking CUE and biomass turnover is to describe how each changes in response to biomass increments. Sinsabaugh et al. (2015) found that growth increased with biomass with an exponent of approximately 0.75 ($R^2 \approx 0.6$) for both bacteria and fungi. To estimate growth (μ) from biomass, we normalized this regression to our data (i.e. shifted the intercept) by assuming a specific growth rate of 0.001/h at mean biomass concentration (62.2 □mol C/g), based on a mean qCO_2 of 0.003/h for soil microbes (Spohn 2015) and a mean CUE of 0.25. Because production rate scales sublinearly (~0.75) with biomass, biomass turnover time increases as biomass increases. CUE also increases with biomass but the scaling coefficient is smaller (~0.30, Fig. 6a). When directly compared, the net effect is that

This article is protected by copyright. All rights reserved.

Accepted Article

biomass specific turnover time and biomass specific CUE have a scaling coefficient of 0.509 ± 0.041 ($\delta(\ln T_B) / \delta(\ln CUE)$, Fig. 7b).

A coefficient of about 0.5 is implicit in the regression models presented by Sinsabaugh et al. (2015) because production rate was proportional to $B^{0.75}$ and CUE was proportional to $B^{0.25}$. But unlike the earlier study, the CUE values in the current study (Fig. 7b) are independent of the biomass turnover estimates because CUE was calculated from stoichiometric parameters (eq. 2) while the biomass turnover rates were generated from a growth vs. biomass regression.

Nutrient use efficiency

An inverse relationship between CUE and nutrient use efficiency is intrinsic to the stochiometric model presented in equation 2. Because C supplies both the energy and the mass for growth, the upper limit for CUE is about 0.6. This constraint does not apply to N or P use efficiency (NUE, PUE). If NUE or PUE can range to 1.0, then eq. 2 can be rearranged as:

$XUE_{X:C} = XUE_{max}[S_{X:C}/(S_{X:C} + K_C)]$, where $S_{X:C} = (1/EEA_{X:C})(B_{X:C} / L_{X:C})$ [5]

where X represents N or P, $K_C = 0.5$ and $XUE_{max} = 1.0$. From eq. 5, the mean NUE and PUE values for our data were 0.804 ± 0.137 (SD) and 0.814 ± 0.145, respectively (Table 2, Fig. 8).

Carbon use efficiency and geographic variables

We used structural equation models to assess whether the local variables used to calculate CUE were correlated with a broader set of geographic variables. For the full data set, latitude, MAT and MAP were highly correlated (latitude and MAT r = -0.94, latitude and MAP r = -0.71, MAT and MAP r = 0.66) with much weaker correlations with soil pH ($r < |0.1|$) (Fig. 9). None of these variables had strong direct links to $CUE_{C:N}$ ($R^2 < 0.05$). The CUE component variables were also highly correlated as presented above. For the standardized variables in the SEM, the strongest correlations were between BG and NAG+LAP (r=0.88) and $B_{C:N}$ and $L_{C:N}$ (r=0.40).

This article is protected by copyright. All rights reserved.

Accepted Article

The *post hoc* SEM (Fig. 8) deleted three paths relative to the *a priori* model (latitude → NAG+LAP, MAT → $L_{C:N}$, pH → $B_{C:N}$, Likelihood Ratio for nested *post hoc* model p=0.14, $\chi 2$ = 666, df = 19, n=1827, p<0.001). The strongest regression coefficients for the ecosystem to enzyme paths were latitude → BG (-0.20) and MAT → BG (-0.35, Table 3). The strongest paths from geographic variables to elemental ratios were latitude → $L_{C:N}$ (0.39) and latitude → $B_{C:N}$ (0.27). In turn, the direct linear paths linking the four $CUE_{C:N}$ component variables to $CUE_{C:N}$ captured 16% of the variance in $CUE_{C:N}$. The actual relationships between these variables and $CUE_{C:N}$ are defined by equation 2 and described by the non-linear correlations presented in Fig. 2.

The *a priori* SEMs for the subset of tropical forest A horizon soils (Turner, Table S2) did not include MAT as a variable because all sites had a MAT of 26C. The strongest correlation among ecosystem variables was between latitude and MAP (r = 0.88). The correlations among the $CUE_{C:N}$ component variables were weaker than those in the global model, with the greatest correlation between BG and NAG+LAP (r=0.54). The reduced *post hoc* model deleted four paths (pH → NAG+LAP, MAP → $L_{C:N}$, Latitude → $L_{C:N}$, pH → $B_{C:N}$, Likelihood Ratio for nested *post hoc* model p=0.115, $\chi 2$ = 64.7, df = 24, n=657, p<0.005). The three geographic variables had moderate to strong path coefficients for all of the $CUE_{C:N}$ component variables ($|0.13\ -0.38|$, Table 3). In turn, the direct linear paths linking the four $CUE_{C:N}$ component variables to $CUE_{C:N}$ captured 86% of the variance in $CUE_{C:N}$ (Fig. S1).

For the same subset of tropical forest A horizon soils (Turner, Table S2), the strongest correlation among the $CUE_{C:P}$ component variables was between phosphatase activity and $L_{C:P}$ (r = 0.74). The *post hoc* SEM deleted three paths (latitude → $B_{C:P}$, MAP → BG, latitude → $L_{C:P}$, latitude → phosphatase, Likelihood Ratio for nested *post hoc* model p=0.137, $\chi 2$ = 136.6, df =

This article is protected by copyright. All rights reserved.

15, n=613, p<0.001, Fig. S2). Soil pH had moderate to strong path links to each of the four $CUE_{C:P}$ component variables ($|0.17 – 0.50|$). MAP had strong links to three $CUE_{C:P}$ component variables (AP, $B_{C:P}$ and $L_{C:P}$, 0.24 – 0.48, Table 3). In turn, the direct linear paths linking the four $CUE_{C:P}$ component variables to $CUE_{C:P}$ captured 76% of the variance in $CUE_{C:P}$.

For the subset of North American conifer forest soils (Talbot et al., Table S3), the *a priori* SEM did not include $B_{C:N}$ because these values were not directly measured. The correlations among climatic variables were similar to those for the global model, but the connections between climate variables and soil pH were stronger ($|0.37 - 0.45|$). Among the $CUE_{C:N}$ component variables only BG and NAG+LAP were strongly correlated (r=0.85). The *post hoc* model deleted five paths (MAT → BG, MAP → BG, pH → NAG+LAP, MAP → NAG+LAP, MAT → NAG+LAP, Likelihood Ratio p=0.218, $\chi 2 = 390.6$, df = 26, n=493, p<0.001, Fig. S3), $L_{C:N}$ was linked to all of the ecosystem variables by strong negative regression coefficients (-0.73 to -0.31, Table 3). In turn, the direct linear paths linking the three $CUE_{C:N}$ component variables to $CUE_{C:N}$ captured only 6% of the variance in $CUE_{C:N}$, likely because of the lack of case specific $B_{C:N}$ values (Fig. S3).

Horizon specific SEMs had stronger connections between the geographic and $CUE_{C:N}$ component variables and between the three $CUE_{C:N}$ component variables and $CUE_{C:N}$ (Table 3). The SEM for the O horizon deleted two paths (MAP → NAG+LAP, pH → BG, Likelihood Ratio p=0.218, $\chi 2 = 72.9$, df = 23, n=228, p<0.005, Fig. S4) and captured 31% of the variance in $CUE_{C:N}$. The SEM for the A horizon deleted two paths (MAP → NAG+LAP, MAP → BG, Likelihood Ratio p=0.247, $\chi 2 = 68.9$, df = 23, n=265, p<0.005, Fig. S5) and captured 18% of the variance in $CUE_{C:N}$.

This article is protected by copyright. All rights reserved.

Across the six SEMs, all *post hoc* models included paths from latitude to BG, and pH to $L_{C:N}$ or $L_{C:P}$ (Table 3). Five SEMs included paths from pH to BG and MAP to $L_{C:N}$ (or $L_{C:P}$). The regression coefficients for the pH to $L_{C:N}$ (or $L_{C:P}$) paths were all negative. The coefficients for the MAP to $L_{C:N}$ paths were negative; the MAP to $L_{C:P}$ coefficient was positive (0.32). $B_{C:N}$ and $B_{C:P}$ had the fewest connections to the geographic variables. As expected from eq. 2, all BG to CUE and L to CUE paths had negative coefficients, and all NAG+LAP (or AP) paths to CUE and $B_{C:N}$ (or $B_{C:P}$) to CUE paths had positive coefficients.

There were weak macroscale trends between CUE and both pH and MAT. The relationship between soil pH and CUE was mediated by significant correlations between pH, $L_{C:N}$, $L_{C:P}$ and BG as shown by the structural equation models. CUE generally declined with pH for both conifer and tropical forest soils (for conifer forest $CUE_{C:N}$: -0.0246•pH + 0.3432, R^2=0.041; for tropical forest $CUE_{C:N}$: -0.0197•pH + 0.4001, R^2=0.065; for tropical forest $CUE_{C:P}$: -0.0472•pH + 0.5066, R^2=0.142) (Fig. 10a). When these data sets were excluded, the pH trend for the remaining data reversed, pulled by Aridisols with high pH and high CUE. As a result, the global data showed a CUE minimum at pH 7 (Fig. 10b).

The association between MAT and CUE was more diffuse. While some direct paths between MAT and CUE component variables were significant, it appeared that indirect paths through latitude and MAP to $L_{C:N}$, $L_{C:P}$ and BG were at least as influential. Within the conifer forest data set, ln(CUE) increased with MAT (0.0154/degC ± 0.0075 (95% CI), corresponding to an apparent activation energy of 0.101 ± 0.51 eV as estimated by the Arrhenius equation, Fig. 11). The broader data set showed a similar trend (0.0150/degC ± 0.0053, apparent activation energy of 0.119 ± 0.036 eV). The tropical forest data were excluded from these analyses because all sites had the same MAT of 26C.

This article is protected by copyright. All rights reserved.

Accepted Article

Accepted Article

DISCUSSION

Stoichiometric comparisons

Several measures included in our data have been the subject of other meta-analyses. Our mean biomass C:N ratio of 7.91 ± 0.05 (SE) for soil microbiota approximated the values of 8.6 ± 0.3 (SE) calculated by Cleveland and Liptzin (2007) and 7.6 (no error estimate provided) reported by Xu et al. (2013). For 45 taxa of Ascomycota, Basidiomycota and Zygomycota isolated from grassland litter, the mean C:N ratio was 8.3 ± 1.1 (95% CI); for 42 cultures of Actinobacteria, Proteobacteria and Bacteriodetes from the same litter the C:N ratio was 6.1 ± 0.6 (Mouginot et al. 2014). The mean $EEA_{C:N}$ ratio for our data set (1.335 ± 0.053, 95% CI) was similar to that reported for terrestrial soils by Sinsabaugh and Follstad Shah (2012) (1.434 ± 0.220, 95% CI). Mean estimates for the ratio of SOC:TN (14.3 from Cleveland and Liptzin (2007) and 16.4 from Xu et al. (2013)) were lower than the $L_{C:N}$ mean of 19.6 for our data, which combined measurements from both mineral and organic horizons.

The mean microbial biomass C:P ratio (42.2 ± 1.9, SE) for our largely tropical forest data was lower than the mean of 59.5 ± 3.6 (SE) reported by Cleveland and Liptzin (2007) but similar to the mean of 42 reported by Xu et al. (2013). The $EEA_{C:P}$ ratio of 0.180 ± 0.015 (95% CI) was lower than the mean of 0.617 ± 0.045 reported by Sinsabaugh and Follstad Shah (2012) for a data set dominated by temperate and boreal systems, but similar to the ratio of 0.21 ± 0.05 (95% CI) ratio reported for tropical systems by Waring et al. (2013). The mean ratio of SOC:TP for our tropical sites was 278 ± 20 (95% CI) compared to values of 186 and 287 calculated by Cleveland and Liptzin (2007) and Xu et al. (2013), respectively. However, for the $CUE_{C:P}$ calculations we defined $L_{C:P}$ as the ratio of SOC:SOP. For tropical soils, SOP is approximately 25% of total P (Turner and Engelbrecht 2011). Our mean SOC:SOP value of 1211 and yielded a

This article is protected by copyright. All rights reserved.

mean $CUE_{C:P}$ estimate of 0.252, which approximated the mean $CUE_{C:N}$ estimate of 0.287 for these sites (Table 2). For reference, inflating the apparent bioavailability of P by substituting SOC:TP for $L_{C:P}$ yields a mean $CUE_{C:P}$ value of 0.38, which is inconsistent with the low $EEA_{C:P}$ ratios observed and the generally low bioavailability of P in tropical soils (Vitousek et al. 2010).

The exercise highlights the difficulty of estimating bioavailable P from chemical measures. Our assumption is that much of the organic P is potentially available, which is supported by its chemical composition and apparent dynamic nature over relatively short timescales in tropical forests (Vincent et al. 2010; Turner and Engelbrecht 2011; Turner et al. 2015). This limitation, along with a broader range of biomass C:P composition and uncoupled pathways for C and P uptake, produces greater heteroscedasticity among the $CUE_{C:P}$ component variables, relative to $CUE_{C:N}$ (Figs. 2-3). Despite these problems, the often contrasting values for $CUE_{C:N}$ and $CUE_{C:P}$ converge when normalizing to the N:P ratio of available resources ($L_{N:P}$, Fig. 4).

Frequency distributions of CUE

The frequency distribution of CUE estimates for soil microbial communities was similar to that for freshwater sediments calculated with the same stoichiometric model (Fig. 12). The arithmetic mean CUE for freshwater sediments (0.267 ± 0.087, SD, median also 0.267, n = 2100, Hill et al. 2012) is nearly identical to the mean CUE of terrestrial soil and litter (0.269 ± 0.110, n=2046, median = 0.267, Table 2). A meta-analysis of the CUE of bacterial and fungal dominated communities, calculated from direct measures of microbial growth and respiration, averaged 0.336 ± 0.213 (median 0.281, n=932) for bacteria and 0.326 ± 0.196 for fungi (median 0.296, n=398) (Sinsabaugh et al. 2015). Compared to the stoichiometric CUE estimates, which were normally distributed, the distributions of the direct CUE measures have a negative skew

This article is protected by copyright. All rights reserved.

Accepted Article

(Fig. 12). The stoichiometric estimates are based on a saturating Michaelis-Menten formulation with a fixed maximum CUE of 0.60, based on thermodynamic constraints. Direct estimates of microbial community CUE are unconstrained and vary with methodology, which can lead to apparent CUE values greater than 0.60 (Manzoni et al. 2012, Sinsabaugh et al. 2013).

Threshold element ratio and CUE

Carbon use efficiency and the threshold element ratio are inversely related through biomass composition and apparent assimilation efficiency (eq. 1). Consequently, the TER should decrease as microbial CUE increases unless there are compensatory changes in $B_{C:X}$ and A_X (Fig. 5). In our study, the C:N ratio of soils ($L_{C:N}$) spanned the range of $TER_{C:N}$ estimates, but contrary to theoretical predictions the maximal values for $CUE_{C:N}$ did not occur when $L_{C:N}$ = $TER_{C:N}$. Maximum CUE coincided with $L_{C:N}$ ratios that exceeded the $TER_{C:N}$ by 5-20 (Fig. 5b). One plausible explanation is that the bioavailability of N is greater than indicated by the bulk C:N ratio, given that some organic matter fractions are chemically or physically shielded from microbial access (Fanin et al. 2013, Wagai et al. 2013, Kaiser et al. 2014).

Another consideration is that within the stoichiometric model, CUE is a function of enzyme allocation, which is assumed to reflect the bioavailability of resources, as well as the C:N ratios of biomass and substrate. Conceptually, CUE is maximal when the unit costs of obtaining C and N are minimal (Moorhead et al. 2012). These costs vary with organic matter composition as well as element ratio. The rapid decline in $CUE_{C:N}$ as soil C:N decreases below the TER indicates that the cost of obtaining C from chemically protected soil organic matter (Cotrufo et al. 2013) increasingly exceeds the value of its greater N concentration (Moorhead et al. 2013). Conversely, the cost of obtaining N at C:N ratios in excess of the TER may be mitigated when N (and C) are available in more accessible forms.

This article is protected by copyright. All rights reserved.

Accepted Article

Within our tropical forest data set, soil C:P ratio did not overlap with the $TER_{C:P}$ and there was almost no relationship between $L_{C:P}$ and CUE (Fig. 3b). Biomass C:P ratio was the best predictor of $CUE_{C:P}$, but $B_{C:P}$ ratios were not greater than those observed in other systems. The $EEA_{C:P}$ ratios were lower than those of temperate biomes by a factor of 2-3, indicating greater P limitation but also suggesting that P bioavailability is greater than bulk chemical analyses imply. High P use efficiency and tight P cycling as biomass turns over may limit P losses to the bulk soil pool, thereby attenuating the relationships among $CUE_{C:P}$, $TER_{C:P}$ and bulk estimates of $L_{C:P}$.

Biomass turnover and CUE

Equation 2 relates CUE directly to the C:P and C:N ratios of biomass, but the association was stronger for C:P than C:N ratio (R^2 = 0.6 vs. 0.2, regression coefficients of 0.169 vs. 0.115, Figs. 2-3). This trend also appears in the scaling of CUE and biomass (Fig. 6). CUE increased with microbial biomass C (MBC) with a scaling coefficient ($\delta(\ln CUE/\delta(\ln MBC)$) of 0.302 ± 0.057 (95% CI, Fig. 6a). This coefficient is not significantly different from those reported previously for fungal and bacterial dominated communities that used CUE values calculated from rates of growth and respiration (0.27 ± 0.07 and 0.27 ± 0.03, respectively, Sinsabaugh et al. 2015). A broader comparison of $CUE_{C:N}$ in relation to MBC had a coefficient 0.175 ± 0.035 (95% CI). It is not possible to determine whether the lower value is the result of a including a wider variety of ecosystems or a using a narrower estimation of CUE or both.

CUE increases with microbial biomass C because production increases relative to biomass with a scaling coefficient of approximately 0.75 while the coefficient for respiration is approximately 0.50. Sinsabaugh et al. (2015) interpreted this CUE trend as evidence for proto-cooperative processes that increase metabolic efficiency. However, the trend does not extend to

This article is protected by copyright. All rights reserved.

Accepted Article

other elemental measures of biomass concentration. The scaling coefficient for microbial biomass P (MBP) and CUE was -0.254 ± 0.042 (95% CI, Fig. 6b) and the relationship between CUE and microbial biomass N was not significantly different from zero. The inverse relationship between microbial biomass P and CUE strengthens the correlation between $CUE_{C:P}$ and biomass C:P ratio ($R^2 = 0.6$, Fig. 3c) while the poor relationship between CUE and microbial biomass N weakens the connection between biomass C:N and $CUE_{C:N}$ ($R^2 = 0.2$, Fig. 2c).

The relationship between microbial biomass P and CUE differs from that for microbial biomass C and CUE because cellular P content controls growth rates, i.e. the growth rate hypothesis (Sterner and Elser 2002, Allen and Gillooly 2009). Microbial growth increases with cellular P content because most cellular P is in the form of ribosomal RNA (Allen and Gillooly 2009). In turn, the capacity of a cell to respond quickly to environmental resource pulses is linked to rRNA gene copy number, i.e. the capacity to quickly produce new ribosomes (Stevenson and Schmidt 2004, Gyorfy et al. 2015). These traits are advantageous in environments with generally high, but fluctuating, resource availabilities. As examples, Mouginot et al. (2014) isolated bacteria and fungi from decomposing grass litter. For bacteria, but not fungi, growth rates in culture were inversely related to biomass C:N and C:P ratios. DeAngelis et al. (2014) analyzed the bacterial communities from a 20 y soil warming experiment at the Harvard Forest. Average bacterial rRNA gene copy number has decreased with warming, suggesting that the treatment has selected bacteria with a more oligotrophic lifestyle as a result of depletion of labile substrate stocks. Figure 6 suggests that the negative effect of faster growth on CUE is stronger than the positive effect of biomass concentration on CUE.

Biomass turnover and CUE are correlated because both are functions of growth rate, which in turn is connected to the biomass C:P ratio through the growth rate hypothesis. In eq. 2,

This article is protected by copyright. All rights reserved.

Accepted Article

$B_{C:P}$ is one of variables used to calculate CUE; it was also the variable that was most closely correlated with $CUE_{C:P}$ (Fig. 3c). This association may act to attenuate the correlation between $CUE_{C:N}$ and $CUE_{C:P}$.

Only three studies included data on microbial biomass and respiration from which biomass turnover times could be calculated (Fig. 7a). Extrapolating from this limited data to the full data set yielded a mean microbial biomass turnover time of 67 ± 22 d (SD). For comparison, a meta-analysis of fungal biomass turnover based on direct measurements of biomass, growth and respiration had arithmetic mean and median turnover times of 90 and 47 d, respectively (Sinsabaugh et al. 2015).

Turnover time and CUE both increased with biomass with a relative scaling coefficient ($\delta(\ln T_B) / \delta(\ln CUE)$, Fig. 7b) of 0.509 ± 0.041. A similar relationship was reported by Sinsabaugh et al. (2015) using CUE data calculated from growth and respiration measurements. This empirical relationship is significant for process models because it shows that CUE, which determines the fraction of assimilated C that is retained in the soil, and biomass turnover, which determines the transfer of C into soil organic matter pools, are both functions of biomass as well as growth, and biomass is much more often measured.

Nutrient use efficiency

Using eq. 5, the mean NUE value for our data was 0.804 ± 0.137 (SD, Table 2, Fig. 8). Mooshammer et al. (2014) estimated microbial community NUE across a range of substrates from plant litter to organic soil to mineral soil by comparing the uptake of free amino acids to the release of ammonium, finding mean NUEs of 0.70, 0.83 and 0.89, respectively. NUE was a saturating function of $L_{C:N}/B_{C:N}$ best described by a Michaelis-Menten formulation: $NUE = 1.03*(L_{C:N}/B_{C:N})/(0.92 + L_{C:N}/B_{C:N})$, $R^2=0.431$, n=71). Using our data, the Moosehammer et al.

This article is protected by copyright. All rights reserved.

equation yielded a mean NUE similar to that predicted from eq. 5 (0.746 ± 0.096), but the predicted NUE estimates were not well correlated with those estimated from eq. 5 ($y = 0.3062x + 0.5002$, R^2=0.192, n=2046), in part because eq. 5 combines ecoenzymatic and elemental stoichiometry. In addition, the Mooshammer et al. model with our data predicted a minimum NUE of 0.50 at CUE = 0 while eq. 5 predicts that NUE = 1 at CUE = 0 (Fig. 8). Despite these issues, both models yield a similar range of NUE estimates within the CUE range that includes 80% of observed values.

We are not aware of any direct estimates of PUE for microbial communities. While C and N uptake are coupled through the consumption of amino acids and amino sugars, P is assimilated independently of C, mostly by membrane associated symport proteins (Plassard et al. 2011, Dick et al. 2014). From eq. 5, the mean PUE for our data (0.814 ± 0.145, SD, Table 2, Fig. 8) was similar to the mean NUE. Based on eq. 1, the apparent assimilation efficiencies for N and P were also similar (0.66 and 0.69, respectively, Table 2). In the context of our stoichiometric model, these similarities arise because the environmental scarcity of P relative to N is offset by increased ecoenzymatic activity directed toward P acquisition relative to activity directed toward N acquisition.

Large-scale trends in CUE

Microbial CUE is an integrative measure of local resource availability and physicochemical constraints on growth. At larger scales, gradients in resources, climate, and dominant vegetation select community composition, but the connections to community function are tenuous (Talbot et al. 2014). Regressions relating CUE directly to latitude, MAT, MAP or soil pH had R^2 statistics <0.1. For this reason, structural equation modeling was used to

This article is protected by copyright. All rights reserved.

determine whether there were significant trends between geographic variables and the constituent variables that define CUE.

Among its component variables, CUE was most closely correlated to the stoichiometry of the ecoenzymatic activities that mediate C and nutrient acquisition. All six SEMs included significant paths from latitude to ß-glucosidase, five models included paths from pH to ß-glucosidase, and four models had paths from latitude to NAG+LAP (Fig. 9, Figs. S1-S5). For the elemental stoichiometry components of CUE, all models included paths from soil pH to $L_{C:N}$ or $L_{C:P}$, five models had paths from MAP to $L_{C:N}$ or $L_{C:P}$, and four models had paths from latitude to $L_{C:N}$. Biomass composition had the fewest connections to ecosystem variables, suggesting that biomass stoichiometry, a measure of homeostasis, was more constrained than other CUE component variables. However, for many studies, including the subset of conifer forest data, there were no direct measurements of biomass composition, which made it less likely that significant paths would emerge.

Cleveland and Liptzin (2007) did not detect latitudinal trends in microbial biomass C:N and C:P in their meta-analysis, but Xu et al. (2013) found that biomass C:N and C:P ratios varied across biomes in relation to soil organic matter content. In contrast, elemental composition of phytomass does vary with climate and soil nutrient concentration. Foliar C:N and C:P ratios tend to decrease, and N:P ratios increase, with decreasing latitude and increasing MAT and MAP (McGroddy et al. 2004, Reich and Oleksyn 2004, Zechmeister-Boltenstern et al. 2015). Within our global structural equation model, $L_{C:N}$ also decreased with latitude (0.35) and increased with MAP (-0.08). Biome specific models for conifer and tropical forests also showed inverse relationships between $L_{C:N}$ and MAT and MAP, but also for latitude. However, the latitude ranges in these models were small compared to the global range.

This article is protected by copyright. All rights reserved.

Accepted Article

Temperature and pH are often highlighted as master variables ordering the composition and function of microbial communities. The idea that rising temperature per se increases microbial community respiration relative to production, thereby reducing CUE, is common in the ecological literature, but difficult to demonstrate at large spatiotemporal scales where temperature is conflated with resource gradients and shifts in microbial community composition (see discussions by Davidson et al. 2006, Lopez-Urrutia and Moran 2007, Sarmento et al. 2010, Billings and Ballantyne 2013, Wagai et al. 2013). At the biochemical scale, there is no evidence that the activation energy of microbial catabolic pathways is intrinsically different from that of anabolic pathways (Sarmento et al. 2010, Lopez-Urrutia and Moran 2007, Doi et al. 2010). A complication is that growth rate increases with both temperature and resource availability, and CUE is inversely related to growth.

However, our meta-analysis showed a positive trend for $CUE_{C:N}$ and MAT (0.0150/degC ± 0.0053, apparent activation energy of 0.119 ± 0.036 eV, Fig. 10) for both the global data and the subset of conifer forest data. Because CUE was calculated from a stoichiometric model, the CUE effect is driven by gradients in resource availability and ecoenzymatic activity rather than direct temperature effects on respiration and growth. Regression analysis showed that the $EEA_{C:N}$ ratio tended to decrease with MAT (R^2=0.06) while the $B_{C:N}/L_{C:N}$ ratio tended to increase (R^2=0.01). Both effects contribute to greater CUE, so it appears that greater CUE reflects greater resource availability at lower latitudes, which could be a result of increasing rates of net primary production.

Except for tropical forest BG activity, the paths from soil pH to ecoenzymatic activities had negative coefficients. A meta-analysis of soil enzyme activities found that NAG and AP activities generally decreased as soil pH increased with regression coefficients of -0.54 and -0.25,

This article is protected by copyright. All rights reserved.

Accepted Article

respectively while LAP activity increased (1.25); BG activity did not vary significantly (Sinsabaugh et al. 2008).

For soils with pH<7, both $CUE_{C:N}$ and $CUE_{C:P}$ were inversely related to pH suggesting that resources decline, or alternatively that growth rates increase (Fig. 10). For tropical forest data, the $EEA_{C:P}$ ratio increased exponentially with increasing pH from about 0.1 to 0.6 (exp = 0.66, R^2=0.41), indicating lower P limitation and faster growth at circumneutral pH. $B_{C:P}/L_{C:P}$ followed a similar, but weaker trend (exp= 0.27, R^2=0.10). A similar pattern occured for $CUE_{C:N}$; $EEA_{C:N}$ increased exponentially with pH, depressing CUE (exp=0.17, R^2=0.15). But $B_{C:N}/L_{C:N}$ remained flat. For the conifer data, both $EEA_{C:N}$ and $B_{C:N}/L_{C:N}$ increased with pH, but similar to the tropical forest C:P data, the effect was greater for $EEA_{C:N}$ so $CUE_{C:N}$ declined ($EEA_{C:N}$ exp=0.30, R_2=0.10. $B_{C:N}/L_{C:N}$ exp=0.10, R^2=0.06). For arid soils, the $CUE_{C:N}$ trend reversed as pH increased beyond 7.0, consistent with slower growth.

Underlying these stoichiometric trends is the relationship between pH and the relative abundance and growth of fungi and bacteria. Fungal C:N ratio is greater than that of bacteria (Strickland and Rousk 2010, Mouginot et al. 2014), which can increase CUE. Fungal biomass and growth decline, and respiration increases, as soil pH increases from 4 to 7 (Rousk et al. 2010), which directly reduces CUE. Conifer forest soils with ectomycorrhizal-dominated fungal communities showed the same pattern as tropical forest soils with arbuscular-mycorrhizal dominated fungal communities (Fig. 10A). Lauber et al. (2008) found that soil pH was the best predictor of bacterial community composition while fungal community composition was most closely associated with changes in soil nutrient availability, specifically extractable P and soil C:N ratio. The upturn in CUE with alkaline pH is associated with arid soils. In these systems, much of the soil surface is colonized by biological crusts composed of primary producers in the

This article is protected by copyright. All rights reserved.

Accepted Article

form of mosses, lichens and cyanobacteria in symbiotic association with fungi (Pointing and Belnap 2012).

Conclusions

Carbon use efficiency and microbial biomass turnover are critical parameters for mechanistic models of soil C dynamics. Our analyses show that values predicted from stoichiometric models are generally similar to those reported from direct measurements of rates, although we have no examples where both approaches have been applied to the same soil samples. Because stoichiometric data are broadly available, the utility of ecosystem models can potentially be improved by adopting site- and season-specific parameters for microbial CUE and biomass turnover based on the empirical relationships presented. At larger scale, the growing body of stoichiometric data makes it possible to resolve patterns in CUE along resource gradients associated with mean annual temperature and soil pH. The existence of such gradients as bases for predicting long-term responses to climate drivers is a topic of considerable interest and debate.

The low congruence of CUE values derived from C:N and C:P models highlights the problem of representing C and nutrient bioavailability using bulk chemical analyses, especially in the case of P. Calculations based on analyses of potentially more labile organic matter pools such as soil solution or soil extracts may lead to better correspondence. Like C use efficiency, the use efficiencies of N and P are critical parameters for biogeochemical models of soil processes. These values can be predicted from our stoichiometric model, but are difficult to independently verify. Despite data gaps and methodological diversity, the integration of stoichiometric and metabolic models provides a quantitative description of the functional

This article is protected by copyright. All rights reserved.

Accepted Article

organization of soil microbial communities in relation to edaphic variables that can improve the representation of CUE in microbial process and ecosystem simulation models.

ACKNOWLEDGEMENTS

BGW and JSP thank an NSF CAREER grant DEB-1053237 (to JSP). CRK and RLS were supported by a Science Focus Area grant to Los Alamos National Laboratory by the US Department of Energy, Office of Science, Biological and Environmental Research Division.

LITERATURE CITED

Allen, A.P., and J.F. Gillooly. 2009. Towards and integration of ecological stoichiometry and the metabolic theory of ecology to better understand nutrient cycling. Ecology Letters 12:369–384.

Allison, S.D., and P.M. Vitousek. 2005. Responses of extracellular enzymes to simple and complex nutrient inputs. Soil Biology & Biochemistry 37:937-944.

Bar-Even, A., E. Noor, Y. Savir, W. Liebermeister, D. Davidi, D.S. Tawfik, and R. Milo R. 2011. The moderately efficient enzyme: Evolutionary and physicochemical trends shaping enzyme parameters. Biochemistry 50:4402-4410.

Billings, S.A., and F. Ballantyne. 2013. How interactions between microbial resource demands, soil organic matter stoichiometry, and substrate reactivity determine the direction and magnitude of soil respiratory responses to warming. Global Change Biology 19:90–102.

This article is protected by copyright. All rights reserved.

Accepted Article

Accepted Article

Bradford, M.A., and T.W. Crowther. 2013. Carbon use efficiency and storage in terrestrial ecosystems. New Phytologist 199:7-9.

Bradford, M.A., A.D. Keiser, C.A. Davies, C.A. Mersmann, and M.S. Strickland. 2013. Empirical evidence that soil carbon formation from plant inputs is positively related to microbial growth. Biogeochemistry 113: 271–281.

Burns, R.G., J.L. DeForest, J.C. Marxsen, R.L. Sinsabaugh, M.E. Stromberger, M.D. Wallenstein, M.H. Weintraub, and A. Zoppini. 2013. Soil enzyme research: current knowledge and future directions. Soil Biology & Biochemistry 58:216-234.

Cherif, M., and M. Loreau. 2007. Stoichiometric constraints on resource use, competitive interactions, and elemental cycling in microbial decomposers. American Naturalist 169:709-724.

Clemmensen, K.E., A. Bahr, O. Ovaskainen, A. Dahlberg, A. Ekblad, H. Wallander, J. Stenlid, R.R. Finlay, D.A. Wardle, and B.D. Lindahl. 2013. Roots and associated fungi drive long-term carbon sequestration in boreal forest. Science 339:1615-1618.

Cleveland, C.C., and D. Liptzin. 2007. C:N:P stoichiometry in soil: Is there a “Redfield ratio” for the microbial biomass? Biogeochemistry 85:235-252.

Cornish-Bowden, A. 2012. Fundamentals of Enzyme Kinetics, 4th ed. Wiley-Blackwell, Weinheim, Germany.

This article is protected by copyright. All rights reserved.

Accepted Article

Cotrufo, M.F., M.D. Wallenstein, C.M. Boot, K Denef, and E. Paul. 2013. The Microbial Efficiency-Matrix Stabilization (MEMS) framework integrates plant litter decomposition with soil organic matter stabilization: do labile plant inputs form stable soil organic matter? Global Change Biology 19:988-995.

Davidson, E. A., I. A. Janssens, and Y. Luo. 2006. On the variability of respiration in terrestrial ecosystems: moving beyond Q10. Global Change Biology 12:154-164.

DeAngelis, K.M., G. Pold, B.D. Topçuoglu, L.T.A. van Diepen, R.M. Varney, J.L. Blanchard, J. Melillo, and S.D. Frey. 2015. Long-term forest soil warming alters microbial communities in temperate forest soils. Frontiers in Soil Microbiology 6: article 104.

Dick, C.F., A.L.A. Dos-Santos, and J.R. Meyer-Fernandez. 2014. Inorganic phosphate uptake in unicellular eukaryotes. Biochimica et Biophysica Acta 1840:2123–2127.

Doi, H., M. Cherif, T. Iwabuchi, I. Katano, J.C. Stegen, M. Striebel. 2010. Integrating elements and energy through the metabolic dependencies of gross growth efficiency and the threshold elemental ratio. Oikos 119:752-765.

Elser, J.J., K. Acharya, M. Kyle, J. Cotner, W. Makino, T. Markow, T. Watts, S.E. Hobbie, W. Fagan, J Schade, J Hood, and R.W. Sterner. 2003. Growth rate-stoichiometry couplings in diverse biota. Ecology Letters 6:936–943.

This article is protected by copyright. All rights reserved.

Accepted Article

Finzi, A.C., R.L. Sinsabaugh, T. M. Long, M.P. Osgood. 2006. Microbial community responses to atmospheric CO2 enrichment in a Pinus taeda forest. Ecosystems 9:215-226.

Frost, P.C., J.P. Benstead, W.F. Cross, H. Hillebrand, J.H. Larson, M.A. Xenopoulos, and T. Yoshida. 2006. Threshold elemental ratios of carbon and phosphorus in aquatic consumers. Ecology Letters 9:774–779.

German, D.P., K.R.B. Marcelo, M.M. Stone, and S.D. Allison. 2012. The Michaelis–Menten kinetics of soil extracellular enzymes in response to temperature: a cross-latitudinal study. Global Change Biology 18:1468–1479.

Green, L.E., A. Porras-Alfaro, and R.L. Sinsabaugh. 2008. Translocation of nitrogen and carbon interates biotic crust and grass production in desert grassland. Journal of Ecology 96:1076-1085.

Gyorfy, Z., G. Draskovits, V. Vernyik, F.F. Blattner, T. Gaal, and G. Posfai. 2015. Engineered ribosomal RNA operon copy-number variants of E. coli reveal the evolutionary trade-offs shaping rRNA operon number. Nucleic Acids Research 43:1783–1794.

Hernandez, D.L., and S.E. Hobbie. 2010. The effects of substrate composition, quantity and diversity on microbial activity. Plant and Soil 335:397-411.

This article is protected by copyright. All rights reserved.

Accepted Article

Hill, B.H., C.M. Elonen, L.R. Seifert, A.A. May, and E. Tarquinio. 2012. Ecoenzymatic stoichiometry and nutrient limitation in US streams and rivers. Ecological Indicators 18:540-551.

Hill, B.H., C.M. Elonen, T.M. Jicha, R.K. Kolka, L.L.P. Lehto, S.D. Sebestyen, L.R. Seifert-Monson 2014a. Ecoenzymatic stoichiometry and microbial processing of organic matter in northern bogs and fens reveals a common P-limitation between peatland types. Biogeochemistry 120:203-224.

Hill, B.H., C.M. Elonen, L.E. Anderson, J.C. Lehrter. 2014b. Microbial respiration and ecoenzyme activity in sediments from the Gulf of Mexico hypoxic zone. Aquatic Microbial Ecology 72:105–116.

Hui, D., M. Mayes, and G. Wang. 2013. Kinetic parameters of phosphatase: A quantitative synthesis. Soil Biology & Biochemistry 65:105-113.

Lauber, C.L., M.S. Strickland, M.A. Bradford, and N. Fierer. 2008. The influence of soil properties on the structure of bacterial and fungal communities across land-use types. Soil Biology & Biochemistry 40:2407–2415.

Lee, Z.M., and T.M. Schmidt. 2014. Bacterial growth efficiency varies in soils under different land management practices. Soil Biology & Biochemistry 69:282-290.

This article is protected by copyright. All rights reserved.

López-Urrutia, A., and X.A.G. Morán. 2007. Resource limitation of bacterial production distorts the temperature dependence of oceanic carbon cycling. Ecology 88:817-822.

Manzoni, S., P. Taylor, A. Richter, A. Porporato,and G.I. Ägren. 2012. Environmental and stoichiometric controls on microbial carbon-use efficiency in soils. New Phytologist 196:79–91.

McGroddy, M.E., T. Daufresne, and L.O. Hedin. 2004. Scaling of C:N:P stoichiometry in forests worldwide: implications of terrestrial Redfield-type ratios. Ecology 85:2390–2401.

Moorhead DL, Lashermes G, Sinsabaugh. RL. 2012. A theoretical model of C- and N-acquiring exoenzyme activities, which balances microbial demands during decomposition. Soil Biology and Biochemistry 53:133-141.

Moorhead, D.L., G. Lashermes, R.L. Sinsabaugh, and M.N. Weintraub. 2013. Calculating co-metabolic costs of lignin decay and their impacts on carbon use efficiency. Soil Biology & Biochemistry 66:17-19.

Mooshammer, M., W. Wanek, I. Hämmerle, L. Fuchschlueger, F. Hofhansl, A. Knoltsch, J. Schnecker, M. Takriti, M. Watzka, B. Wild, K.M. Keiblinger, S. Zechmeister-Boltenstern, and A. Richter. 2014. Adjustment of microbial nitrogen use efficiency to carbon:nitrogen imbalances regulates soil nitrogen cycling. Nature Communications DOI: 10.1038/ncomms4694.

This article is protected by copyright. All rights reserved.

Accepted Article

Muoginot, C., R. Kawamura, K.L. Matulich, R. Berlemont, S.D. Allison, A.S. Amend, and A.C. Martiny. 2014. Elemental stoichiometry of Fungi and Bacteria strains from grassland leaf litter. Soil Biology & Biochemistry 76:278-285.

Plassard, C., J. Louche, M.A. Ali, M. Duchemin, E. Legname, and B. Cloutier-Hurteau. 2011. Diversity in phosphorus mobilisation and uptake in ectomycorrhizal fungi. Annals of Forest Science 68:33-43.

Pointing, S.B., and J. Belnap. 2012. Microbial colonization and controls in dryland systems. Nature Reviews Microbiology 10:551-562.

Reich, P.B., and J. Oleksyn. 2004. Global patterns of plant leaf N and P in relation to temperature and latitude. Proceedings of the National Academy of Sciences USA 101:11001–11006.

Rousk, J., P.C. Brookes, and E. Bååth. 2010. Investigating the mechanisms for the opposing pH relationships of fungal and bacterial growth in soil. Soil Biology & Biochemistry 42:926-934.

Sarmento, H., J.M. Montoya, E. Vásquez-Domínguez, D. Vaqué, J.M. Gasol. 2010. Warming effects on microbial food web processes: How far can we go when it comes to predictions? Philosophical Transactions: Biological Sciences 365:2137-2149.

This article is protected by copyright. All rights reserved.

Accepted Article

Accepted Article

Sinsabaugh, R.L., J. Belnap, J.J. Follstad Shah, B.H. Hill, C.R. Kuske, M.E. Litvak, N. Martinez, D.L. Moorhead, S.G. Findlay, K.A. Kuehn, and D. Warnock. 2014. Extracellular enzyme kinetics scale with resource availability. Biogeochemistry 121:287-304.

Sinsabaugh, R.L., and J.J. Follstad Shah. 2012. Ecoenzymatic stoichiometry and ecological theory. Annual Review of Ecology, Evolution and Systematics 43:313-342.

Sinsabaugh, R.L., J.J. Follstad Shah, S.G. Findlay, K.A. Kuehn, and D.L. Moorhead. 2015. Scaling microbial biomass, metabolism and resource supply. Biogeochemistry 122:175-190.

Sinsabaugh, R.L., C.L. Lauber, M.N. Weintraub, B. Ahmed, S.D. Allison, C. Crenshaw, A.R. Contosta, D. Cusack, S. Frey, M.E. Gallo, T.B. Gartner, S.E. Hobbie, K. Holland, B.L. Keeler, J.S. Powers, M. Stursova , C. Takacs-Vesbach, M. Waldrop, M. Wallenstein, D.R. Zak, and L.H. Zeglin. 2008. Stoichiometry of soil enzyme activity at global scale. Ecology Letters 11:1252-1264.

Sinsabaugh, R.L., S. Manzoni, D.L. Moorhead, and A. Richter. 2013. Carbon use efficiency of microbial communities: Stoichiometry, methodology and modeling. Ecology Letters 16:930-939.

Spohn, M. 2015. Microbial respiration per unit microbial biomass depends on litter layer carbon-to-nitrogen ratio. Biogeosciences 12:817–823.

This article is protected by copyright. All rights reserved.

Sterner, R.W., and J.J. Elser. 2002. Ecological stoichiometry: The biology of elements from molecules to the biosphere. Princeton University, Princeton.

Stevenson, B.S., and T.M. Schmidt. 2004. Life history implications of rRNA gene copy number in *Escherichia coli*. Applied and Environmental Microbiology 70:6670-6677.

Stone, M.M., and A.F. Plante. 2014. Changes in phosphatase kinetics with soil depth across a variable tropical landscape. Soil Biology & Biochemistry 71:61-67.

Strickland, M.S., and J. Rousk. 2010. Considering fungal:bacterial dominance in soils e Methods, controls, and ecosystem implications. Soil Biology & Biochemistry 42:1385-1395.

Talbot, J.M., T.D. Bruns, J.W. Taylor, D.P. Smith, S. Branco, S.I. Glassman, S. Erlandson, R. Vilgalys, H.-L. Liao, M.E. Smith, K.G. Peay. 2014. Endemism and functional convergence across the North American soil mycobiome. PNAS 111:6341-6346.

Turner, B.L., and B.M.J. Engelbrecht. 2011. Soil organic phosphorus in lowland tropical rain forests. Biogeochemistry 103:297-315.

Turner, B.L., and S.J. Wright. 2014. The response of microbial biomass and hydrolytic enzymes to a decade of nitrogen, phosphorus, and potassium addition in a lowland tropical rain forest. Biogeochemistry 117:115–130.

Turner, B. L., J. B. Yavitt, K. E. Harms, M. Garcia, and S. J. Wright. 2015. Seasonal changes in soil organic matter after a decade of nutrient addition in a lowland tropical forest. Biogeochemistry 123:221-235.

This article is protected by copyright. All rights reserved.

Accepted Article

Vincent, A. G., B. L. Turner, and E. V. J. Tanner. 2010. Soil organic phosphorus dynamics following perturbation of litter cycling in a tropical moist forest. European Journal of Soil Science 61:48–57.

Vitousek, P. M., S. Porder, B. Z. Houlton, and O. A. Chadwick. 2010. Terrestrial phosphorus limitation: mechanisms, implications, and nitrogen–phosphorus interactions. Ecological Applications 20:5–15.

Wagai, R., A.W. Kishimoto-Mo, S. Yonemura, Y. Shirato, S. Hiradate, and Y. Yagasaki. 2013. Linking temperature sensitivity of soil organic matter decomposition to its molecular structure, accessibility, and microbial physiology. Global Change Biology 19:1114–1125.

Waring, B.G., R. Adams, S. Branco, and J.S. Powers. 2015. Scale-dependent variation in nitrogen cycling and soil fungal communities along gradients of forest composition and age in regenerating tropical dry forests. New Phytologist doi: 10.1111/nph.13654.

Waring, B.G., S.R. Weintraub, and R.L. Sinsabaugh. 2014. Ecoenzymatic stoichiometry of microbial nutrient acquisition in tropical soils. Biogeochemistry 117:101-113.

Xu, X., P.E. Thornton, and W.M. Post. 2013. A global analysis of soil microbial biomass carbon, nitrogen and phosphorus in terrestrial ecosystems, Global Ecology and Biogeography 22:737–749.

This article is protected by copyright. All rights reserved.

Accepted Article

Accepted Article

Zechmeister-Boltenstern, S., K.M. Keiblinger, M. Mooshammer, J. Peñuelas, A. Richter, J. Sardans, W. Wanek. 2015. The application of ecological stoichiometry to plant–microbial–soil organic matter transformations. Ecological Monographs 185:133-153.

Supplemental Tables and Figures

Table S1. Data and metadata from published sources.

Table S2: Data and metadata for tropical forest sites provided by Turner.

Table S3. Data and metadata for conifer forest sites provided by Talbot et al.

Table S4. Data from Duke forest FACE study provided by Kuske et al. and data from Costa Rica tropical forest sites provided by Waring and Powers.

Figure S1. Structural equation model for microbial carbon use efficiency based on C:N stoichiometry for the tropical forest soils. Data in Table S2.

Figure S2. Structural equation model for microbial carbon use efficiency based on C:P stoichiometry for the tropical forest soils. Data in Table S2.

Figure S3. Structural equation model for microbial carbon use efficiency based on C:N stoichiometry for the conifer forest soils. Data in Table S3.

Figure S4. Structural equation model for microbial carbon use efficiency based on C:N stoichiometry for the conifer forest O horizon soils. Data in Table S3.

Figure S5. Structural equation model for microbial carbon use efficiency based on C:N stoichiometry for the conifer forest A horizon soil. Data in Table S3.

This article is protected by copyright. All rights reserved.

Accepted Article

Tables

Table 1. Distribution of data cases by ecosystem type and soil horizon. Records are data sets that correspond to a specific site or treatment.

Ecosystem	Horizon	Records	Cases
Tropical forest	mineral soil	84	787
	litter/organic	2	22
Arid/semiarid	mineral soil	7	117
	litter/organic	2	17
Temperate grassland	mineral soil	4	66
	litter/organic	3	9
Temperate deciduous forest	mineral soil	12	112
	litter/organic	7	24
Temperate coniferous forest	mineral soil	28	280
	litter/organic	23	234
Boreal forest	mineral soil	7	53
	litter/organic	10	73
Arctic/alpine tundra	mineral soil	7	32
	litter/organic	3	40
Agriculture	mineral soil	16	169

This article is protected by copyright. All rights reserved.

Table 2. Definitions, abbreviations and mean values for parameters associated with carbon use efficiency calculations.

Stochiometric parameter	Abbreviation	Arithmetic mean	Std Dev	Median	Geometric mean	Cases	Range
Labile organic matter C:N ratio	$L_{C:N}$	22.2	14.9	16.7	19.3	2046	4.2 - 185
Microbial biomass C:N ratio	$B_{C:N}$	7.91	2.42	8.60	7.59	2046	1.2 - 44
Ecoenzymatic activity C:N ratio	$EEA_{C:N}$	1.316	1.214	1.022	0.988	2046	0.1 - 20
Carbon use efficiency from C:N data	$CUE_{C:N}$	0.269	0.110	0.267	0.243	2046	0.022 - 0.563
Apparent assimilation efficiency for N	A_N	0.658	0.213	0.667	0.609	2046	0.074 - 1.0
Threshold element ratio for C:N	$TER_{C:N}$	28.8	34.9	17.4	19.0	2046	1.1 - 393
Nitrogen use efficiency	NUE	0.804	0.137	0.834	0.787	2046	0.05 - 0.91
Labile organic matter C:P ratio	$L_{C:P}$	1211	1074	890	897	713	42 - 8962
Microbial biomass C:P ratio	$B_{C:P}$	42.2	49.6	31.5	33.2	700	5 - 309
Ecoenzymatic activity C:P ratio	$EEA_{C:P}$	0.180	0.198	0.124	0.107	707	0.01 - 1.11
Carbon use efficiency from C:P data	$CUE_{C:P}$	0.252	0.125	0.242	0.216	694	0.02 - 0.57
Apparent assimilation efficiency for P	A_P	0.687	0.240	0.714	0.632	696	0.06 - 1.0
Threshold element ratio for C:P	$TER_{C:P}$	138	235	92.3	96.6	694	10 - 3257
Phosphorus use efficiency	PUE	0.814	0.145	0.855	0.797	694	0.17 - 0.99

Accepted Article

This article is protected by copyright. All rights reserved.

Table 3. Regression coefficients for structural equation model paths connecting geographic variables to the component variables used to calculate carbon use efficiency (CUE). Results are shown for six post hoc models: two models that used A horizon data from tropical forests (Table S2) to calculate CUE based on C:P and C:N stoichiometry; three models that used O, A and O+A horizon data from conifer forests to calculate CUE based on C:N stoichometry (Table S3); and a global model that uses data from all sites to calculate CUE based on C:N stoichiometry (Tables S1, S2, S3).

Geographic variable	CUE component variable	Tropical C:P A horizon	Tropical C:N A horizon	Conifer C:N O horizon	Conifer C:N A horizon	Conifer C:N O+A horizon	Global C:N O+A horizon
Latitude	BG	0.10	0.22	0.73	-0.32	0.27	-0.20
	NAG+LAP		-0.22	0.79	-0.32	0.26	
	$L_{C:N}$			-0.75	-0.78	-0.73	0.39
	$B_{C:N}$		0.16				0.27
MAT	BG			0.23	-0.37		-0.35
	NAG+LAP			0.35	-0.37		-0.13
	$L_{C:N}$			-0.52	-0.52	-0.48	
	$B_{C:N}$						-0.12
MAP	BG		-0.13	0.18			-0.09
	AP	0.48					
	NAG+LAP		0.38				-0.1
	$L_{C:P}$	0.32					
	$L_{C:N}$			-0.39	-0.54	-0.46	-0.08
	$B_{C:P}$	0.24					
	$B_{C:N}$		-0.37				-0.17
Soil pH	BG	0.35	0.35		-0.16	-0.14	-0.08
	AP	-0.50					
	NAG+LAP			-0.15	-0.18		-0.10
	$L_{C:P}$	-0.42					
	$L_{C:N}$		-0.33	-0.47	-0.27	-0.31	-0.13
	$B_{C:P}$	-0.17					

This article is protected by copyright. All rights reserved.

Accepted Article

Accepted Article

Figure legends

Figure 1. Frequency distribution of soil microbial carbon use efficiencies (CUE) calculated from stoichiometric C:N and C:P models. The median values for $CUE_{C:N}$ and $CUE_{C:P}$ are 0.27 (n=2046) and 0.24 (n=694), respectively.

Figure 2. Soil microbial carbon use efficiency (CUE) in relation to its component C:N variables. A. The ratio of ecoenzymatic C and N acquisition activities: $CUE = -0.1234 \bullet \ln(EEA_{C:N}) + 0.2498$, $R^2 = 0.79$, n=1037, F= 3829. B. Soil C:N ratio: $\ln(CUE) = -0.01587 \bullet L_{C:N} - 1.0617$ $R^2=0.23$, n=2046, F=602. C. Microbial biomass C:N ratio: $CUE = 0.1148 \bullet \ln(B_{C:N}) + 0.0737$, $R^2=0.195$, n=964, F=232. D. The ratio of biomass C:N and soil C:N: $CUE = 0.1092 \bullet \ln(B_{C:N}/L_{C:N}) + 0.3714$, n=2046, $R^2=0.24$, F=632.

Figure 3. Soil microbial carbon use efficiency (CUE) in relation to its component C:P variables. A. The ratio of ecoenzymatic C and P acquisition activities: $CUE = -0.0739 \bullet \ln(EEA_{C:P}) + 0.0858$, $R^2=0.380$, n=691, F=422. B. Soil C:P ratio: $CUE = 0.0178 \bullet \ln(L_{C:P}) + 0.1327$, n=689, $R^2=0.012$, F=8.0, p=0.0047. C. Microbial biomass C:P ratio: $CUE = 0.169 \bullet \ln(B_{C:P}) - 0.3291$, $R^2 = 0.604$, n=650, F=990. D. The ratio of biomass C:P and soil C:P: $CUE = 0.05585 \bullet \ln(B_{C:P}/L_{C:P}) + 0.43815$, n=694, $R^2 = 0.168$, F=140.

Figure 4. Comparison of CUE estimates from C:N and C:P stoichiometry. A. $CUE_{C:P}$ vs. $CUE_{C:N}$: $CUE_{C:P} = 0.568 \bullet CUE_{C:N} + 0.0911$, $R^2=0.162$, n=690, F=133. B. $CUE_{C:P}$ vs. $CUE_{C:N}$ normalized to the substrate N:P ratio ($L_{N:P}$): $(CUE_{C:P} / L_{N:P}) = 0.9697 \bullet (CUE_{C:N}/ L_{N:P}) + 0.00035$, $R^2=0.792$, n=688, F=2615.

This article is protected by copyright. All rights reserved.

Figure 5. CUE and threshold element ratios. A. $\ln(CUE_{C:N}) = -0.5227 \bullet \ln(TER_{C:N}) + 0.1296$, $R^2=0.86$, n=2021, F=12332. B. $CUE_{C:N}$ in relation to the difference between the C:N ratio of available substrate ($L_{C:N}$) and the threshold element ratio ($TER_{C:N}$). C. $\ln(CUE_{C:P}) = -0.7013 \bullet \ln(TER_{C:P}) + 1.659$, $R^2=0.71$, n=671, F=1640. D. $CUE_{C:P}$ in relation to the difference between the C:P ratio of available substrate ($L_{C:N}$) and the threshold element ratio ($TER_{C:P}$).

Figure 6. Carbon use efficiency in relation to microbial biomass. A. CUE vs. MBC: $\ln(CUE) = 0.302 \bullet \ln(MBC) - 3.373$, 95% CI for slope ±0.067, $R^2 = 0.144$, n=641, F = 108. B. CUE vs. MBP: $\ln(CUE) = -0.254 \bullet \ln(MBP) - 0.395$, 95% CI for slope ±0.056, $R^2 = 0.174$, n=653, F = 137.

Figure 7. Microbial biomass turnover time (T_B) in relation to carbon use efficiency (CUE). A. Turnover time calculated from qCO_2 data: $T_B = -197.98 \bullet CUE + 120.08$, $R^2=0.40$, n=28, F=17.0, p=0.00034. B. Scaling of biomass specific turnover time and CUE: $\ln(T_B/MBC) = 0.509 \bullet \ln(CUE/MBC) + 2.443$, 95% CI for slope ±0.042, $R^2=0.474$, n=641, F=575.

Figure 8. Nutrient use efficiency (XUE), calculated from eq. 5, in relation to carbon use efficiency (CUE), calculated from eq. 2. The relationship follows a polynomial regression: $XUE = -12.922 \bullet CUE^4 + 9.408 \bullet CUE^3 - 3.5401 \bullet CUE^2 - 0.0601 \bullet CUE + 0.9872$, $R^2 = 0.99987$, where XUE is N or P use efficiency. XUE equals CUE at a value of 0.48.

Figure 9. Structural equation model linking microbial carbon use efficiency based on C:N stoichiometry to ecosystem variables (n=1827). The model captures 16% of variance in $CUE_{C:N}$.

Figure 10. Microbial carbon use efficiency (CUE) in relation to soil pH. A. CUE declined with pH for both conifer ($CUE_{C:N} = -0.0246 \bullet pH + 0.3432$, $R^2=0.041$) and tropical forest soils ($CUE_{C:N} = -0.0197 \bullet pH + 0.4001$, $R^2=0.065$; $CUE_{C:P} = -0.0472 \bullet pH + 0.5066$, $R^2=0.142$). B.

This article is protected by copyright. All rights reserved.

Accepted Article

CUE vs. soil pH for all data showing a minimum value at pH 7 (CUE = $0.0099(pH)^2 - 0.1073pH + 0.5416$, R^2=0.023, n=2617).

Figure 11. Microbial carbon use efficiency (CUE) in relation to mean annual temperature (MAT). For the conifer forest soils, $CUE_{C:N}$ increased with MAT (0.0154/degC ± 0.0075 (95% CI), R^2=0.043, n=511, F=23.1). The broader data set showed a similar trend (0.0150/degC ± 0.0053, R^2=0.051, n=816, F=44.1). The tropical forest data were excluded from the analysis because all sites had the same MAT of 26C.

Figure 12. Comparative frequency distributions for microbial community CUE estimates. The aquatic sediment values (n=2100) were calculated from data of Hill et al. (2012) using the same stoichiometric model used for the terrestrial soil calculations (n=2002). The bacterial and fungal distributions are based on direct measures of community growth and respiration (bacteria n=1000, fungal n=400) (Sinsabaugh et al. 2015).

This article is protected by copyright. All rights reserved.

Accepted Article

Accepted Article

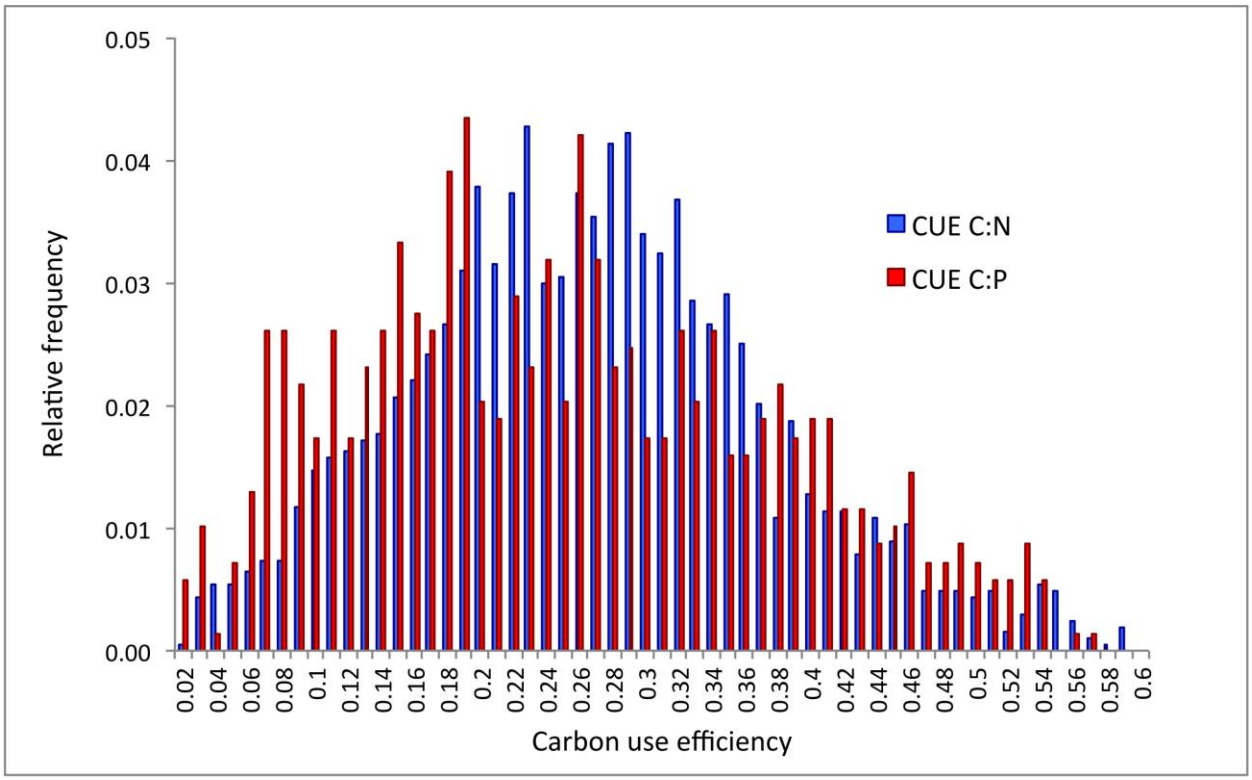

This article is protected by copyright. All rights reserved.

Accepted Article

Figure 2.

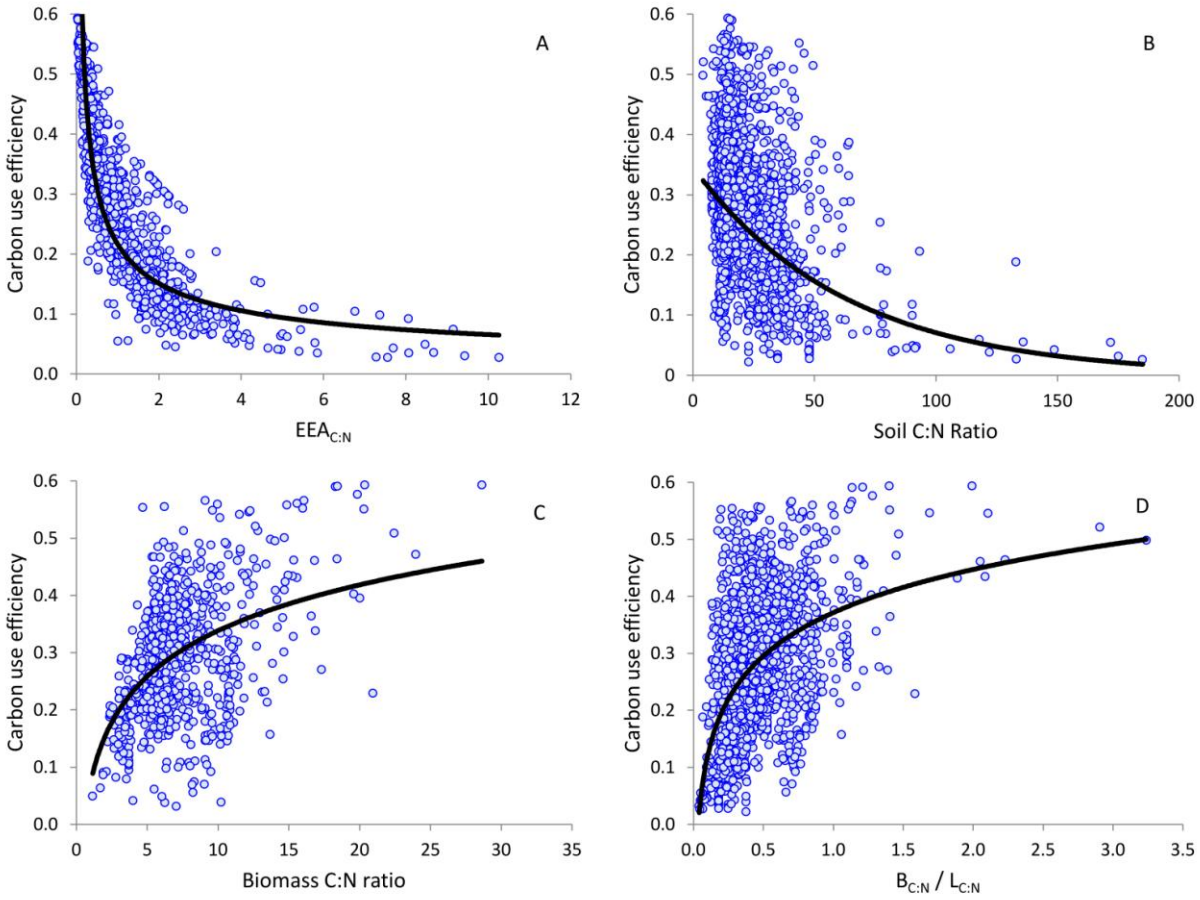

This article is protected by copyright. All rights reserved.

Accepted Article

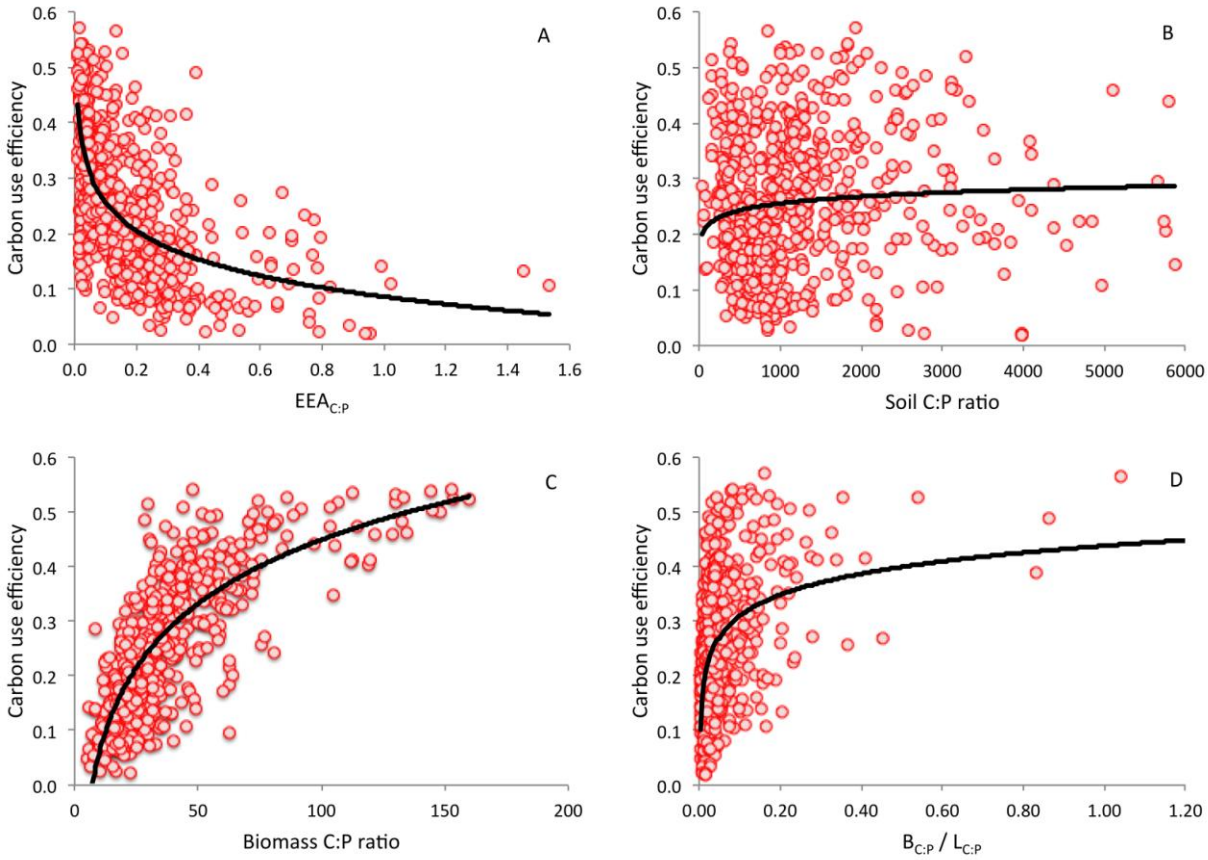

This article is protected by copyright. All rights reserved.

Accepted Article

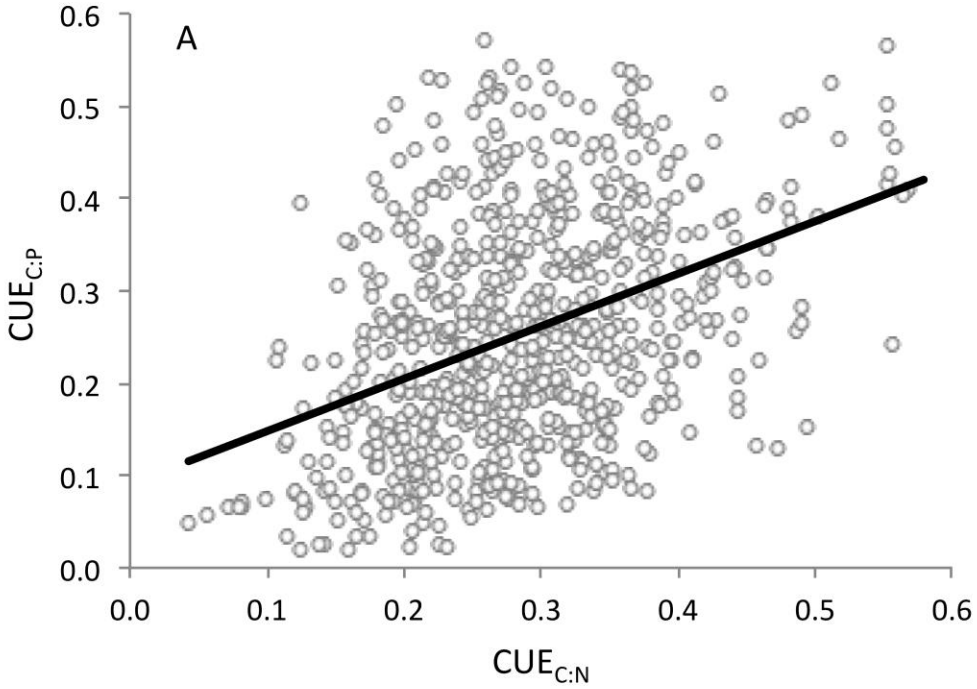

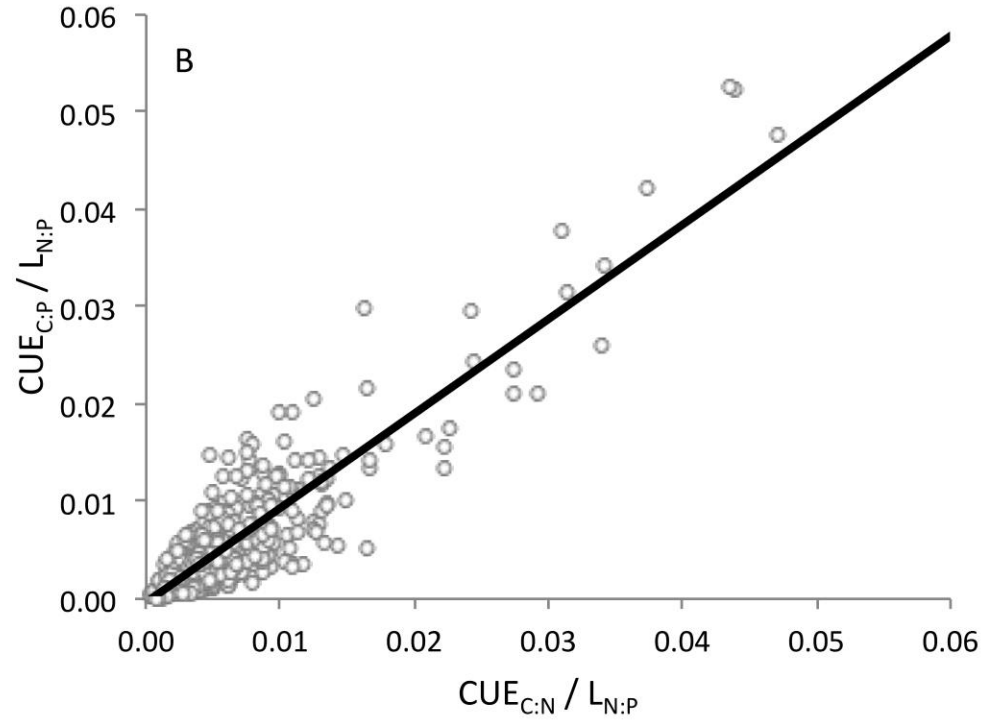

This article is protected by copyright. All rights reserved.

Accepted Article

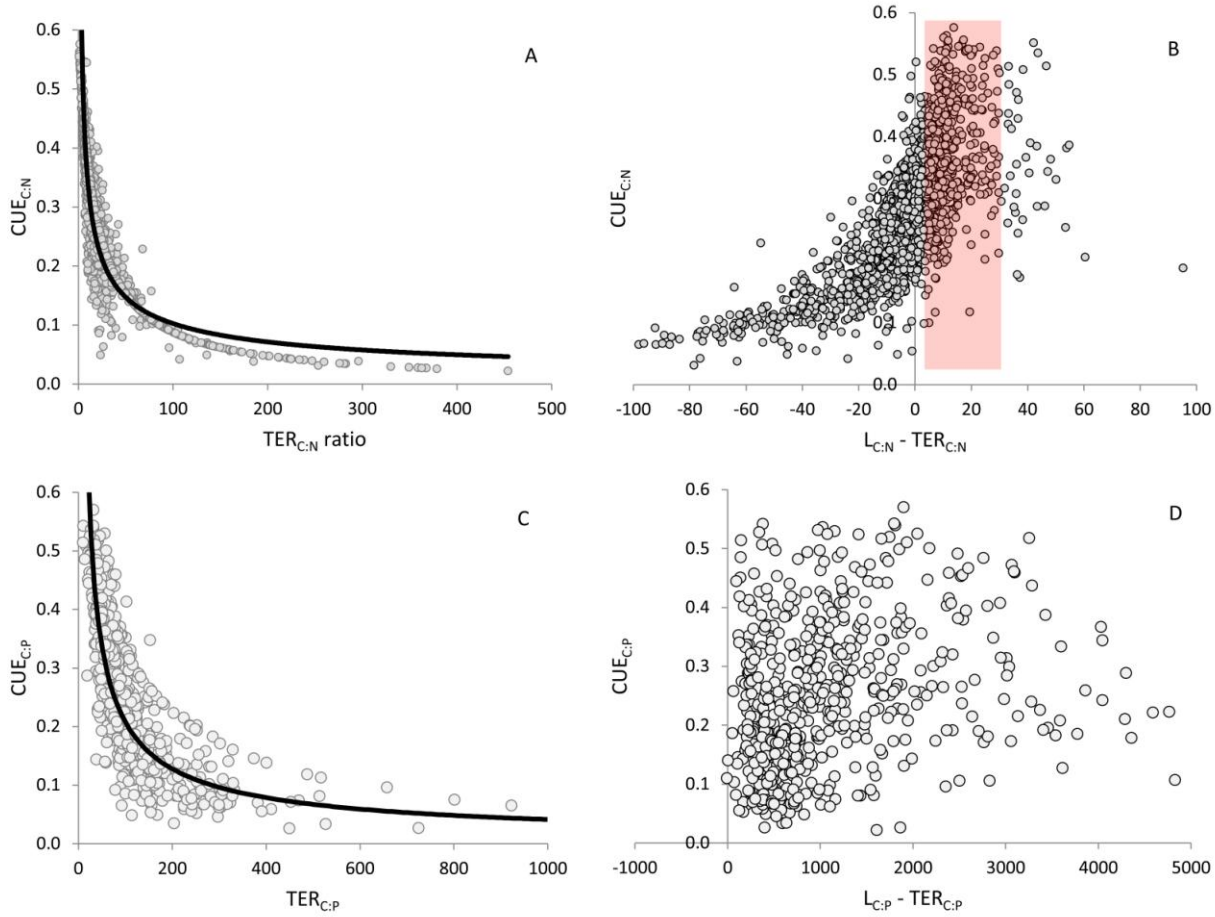

This article is protected by copyright. All rights reserved.

Accepted Article

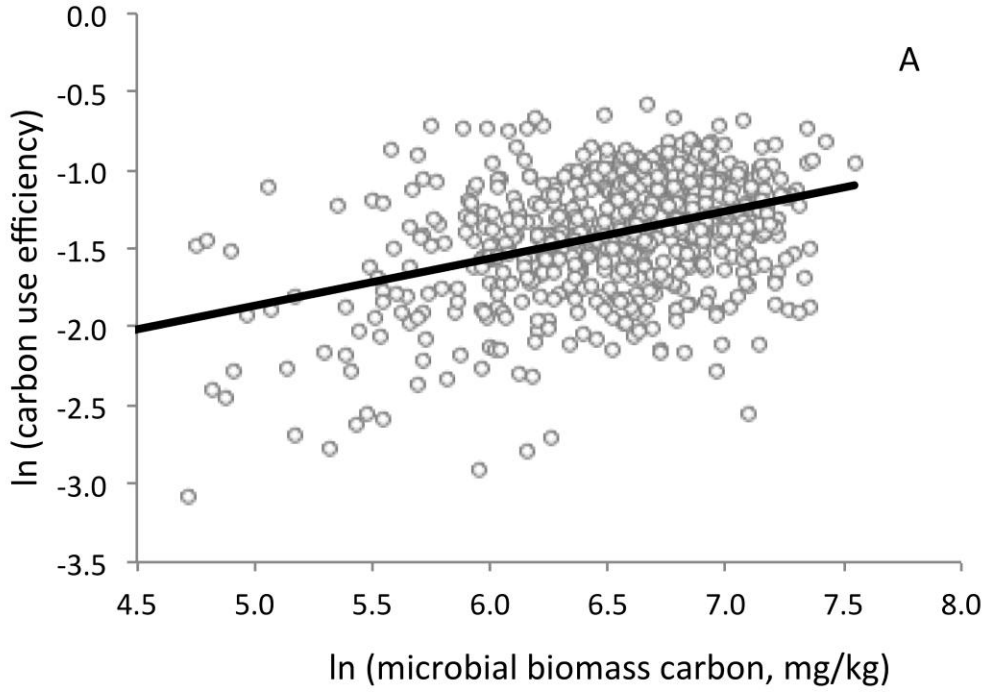

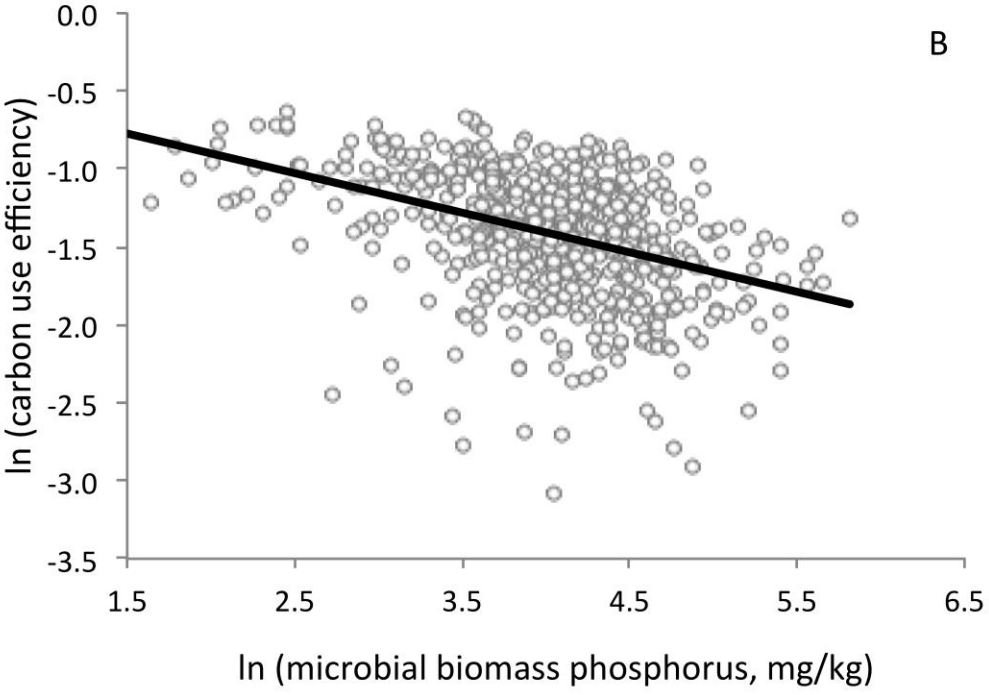

This article is protected by copyright. All rights reserved.

Accepted Article

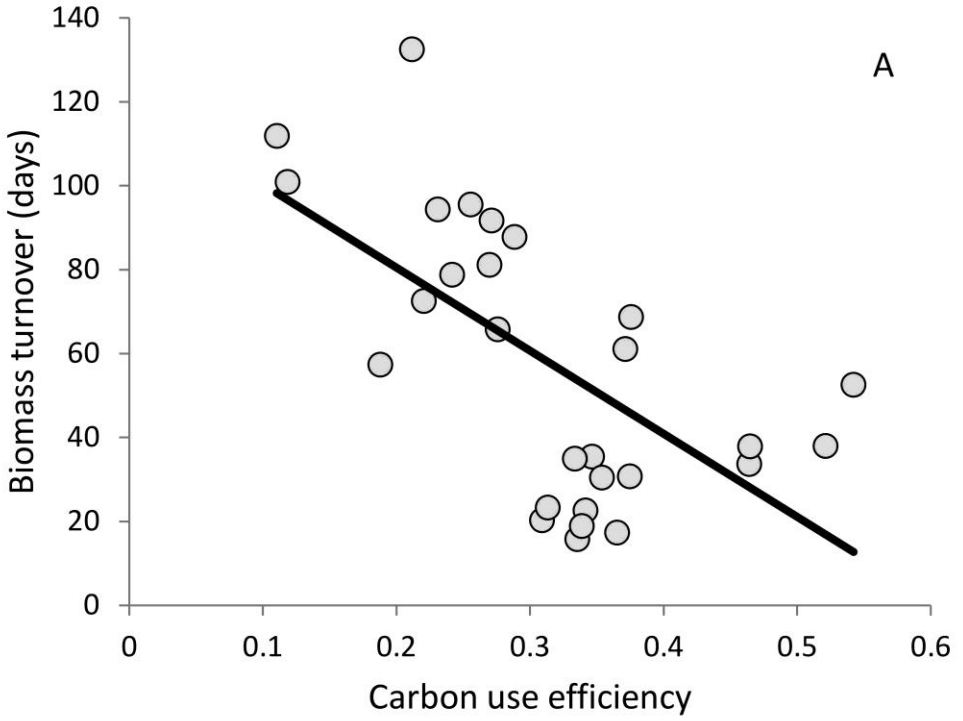

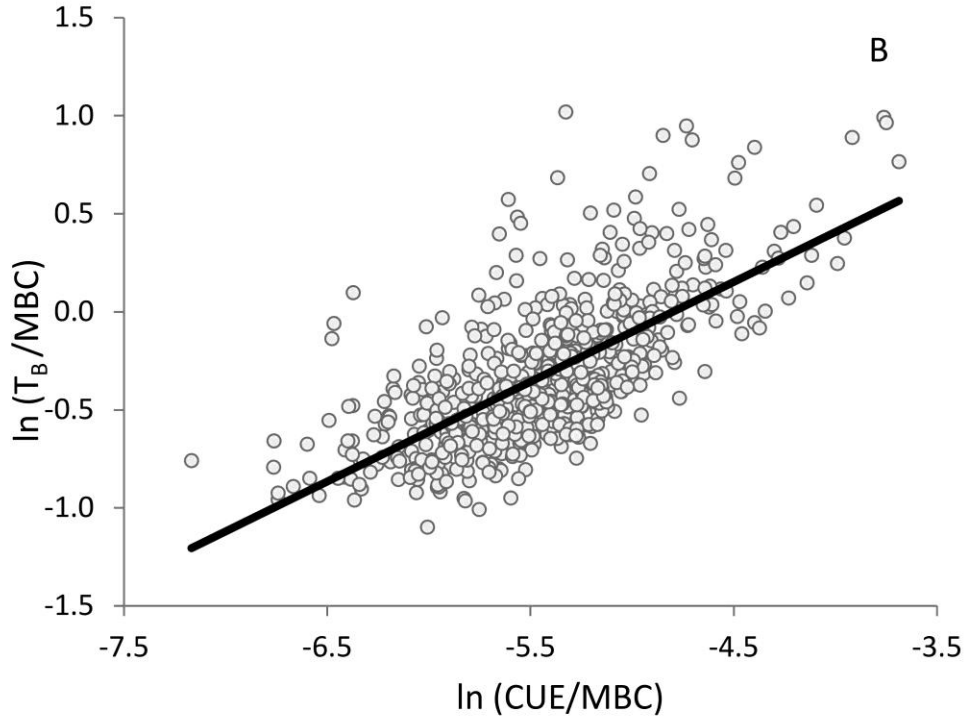

This article is protected by copyright. All rights reserved.

Accepted Article

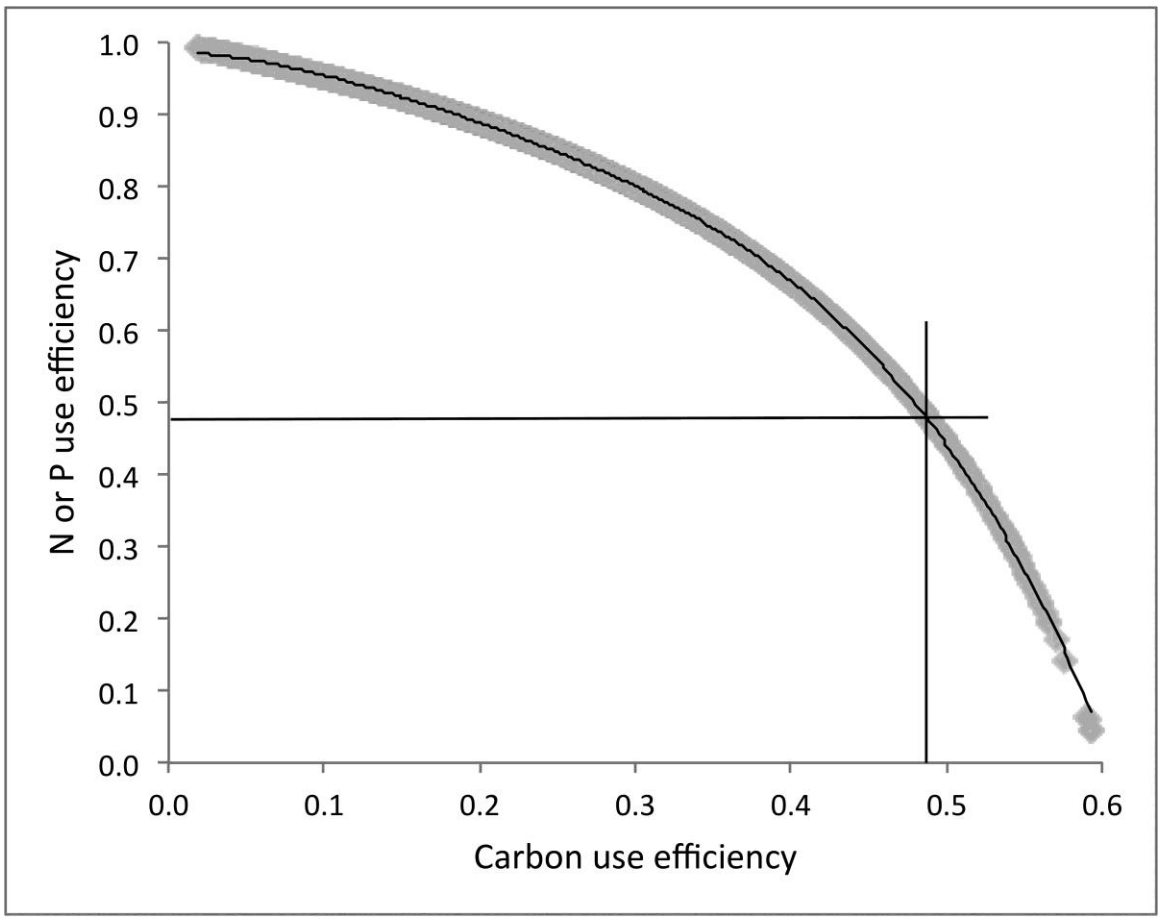

This article is protected by copyright. All rights reserved.

Accepted Article

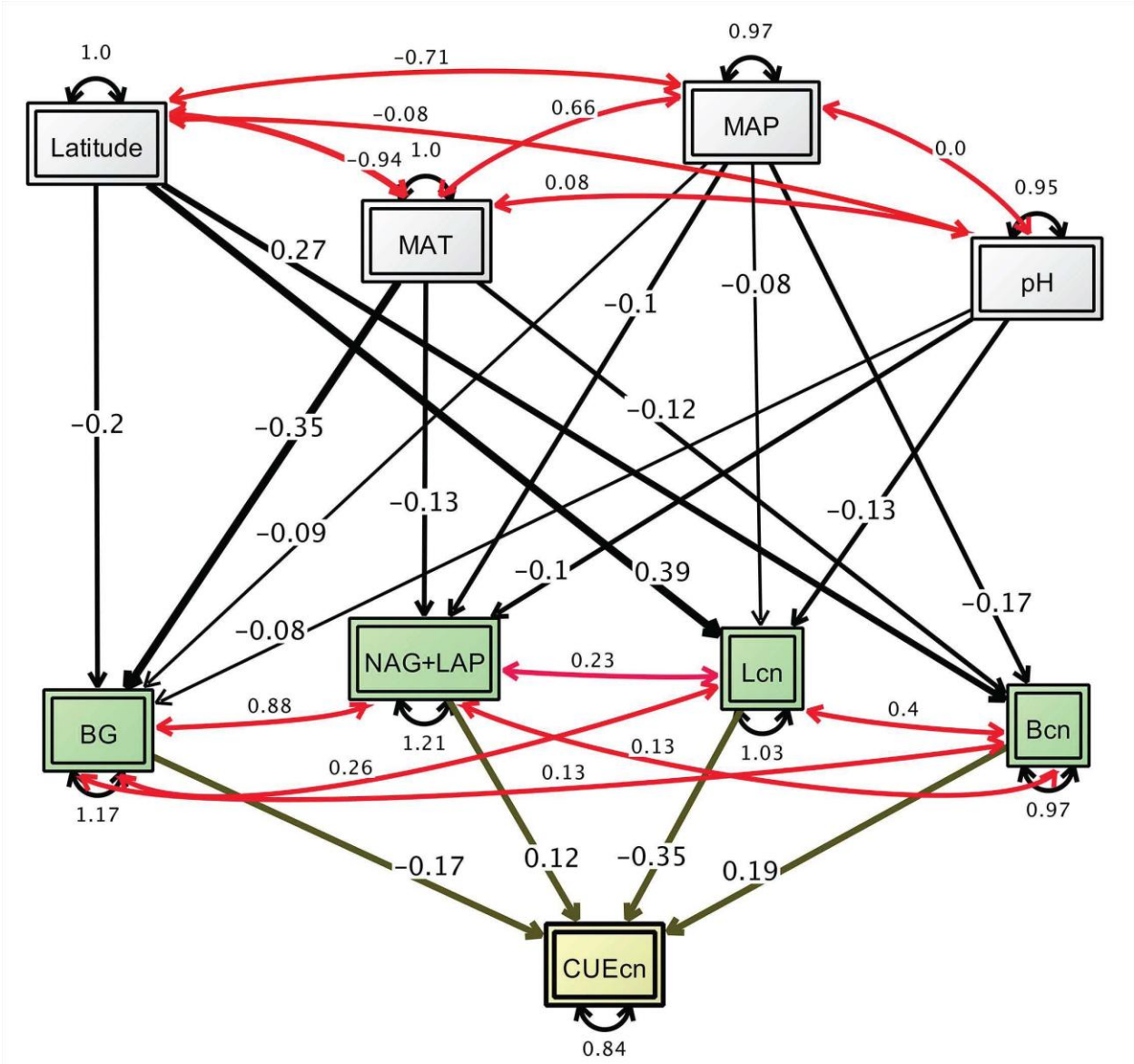

This article is protected by copyright. All rights reserved.

Accepted Article

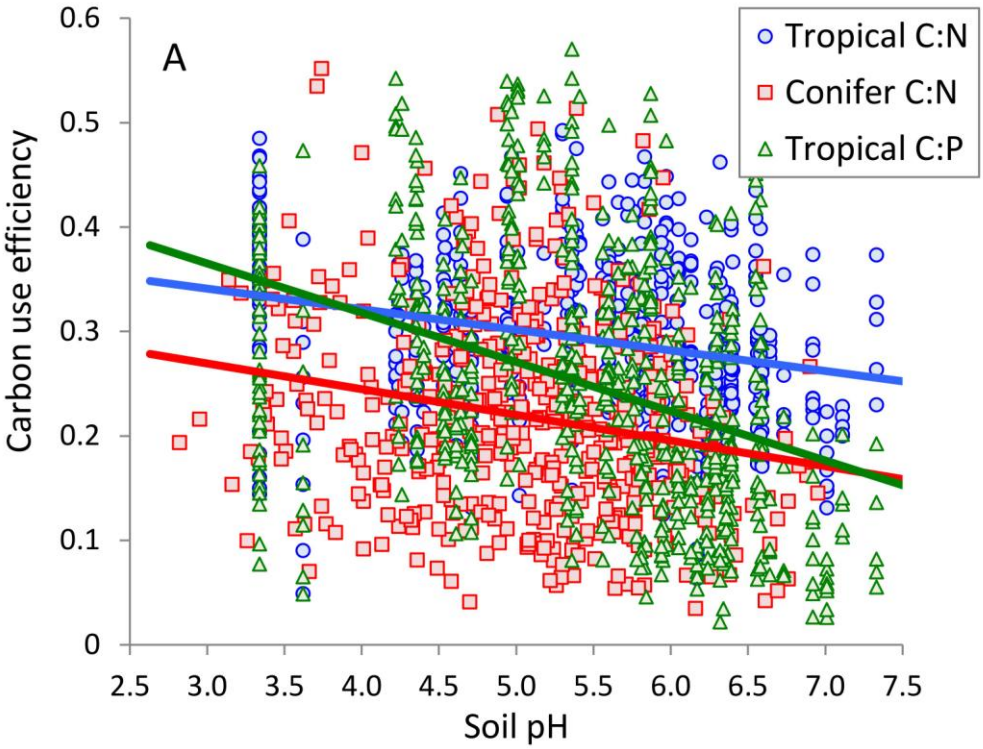

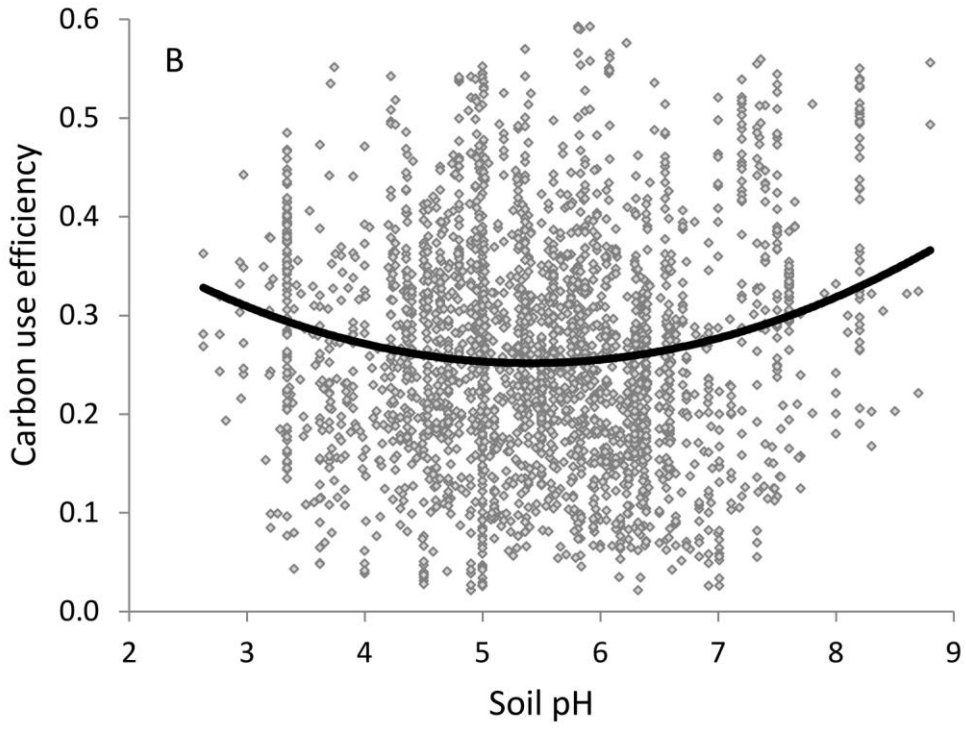

This article is protected by copyright. All rights reserved.

Accepted Article

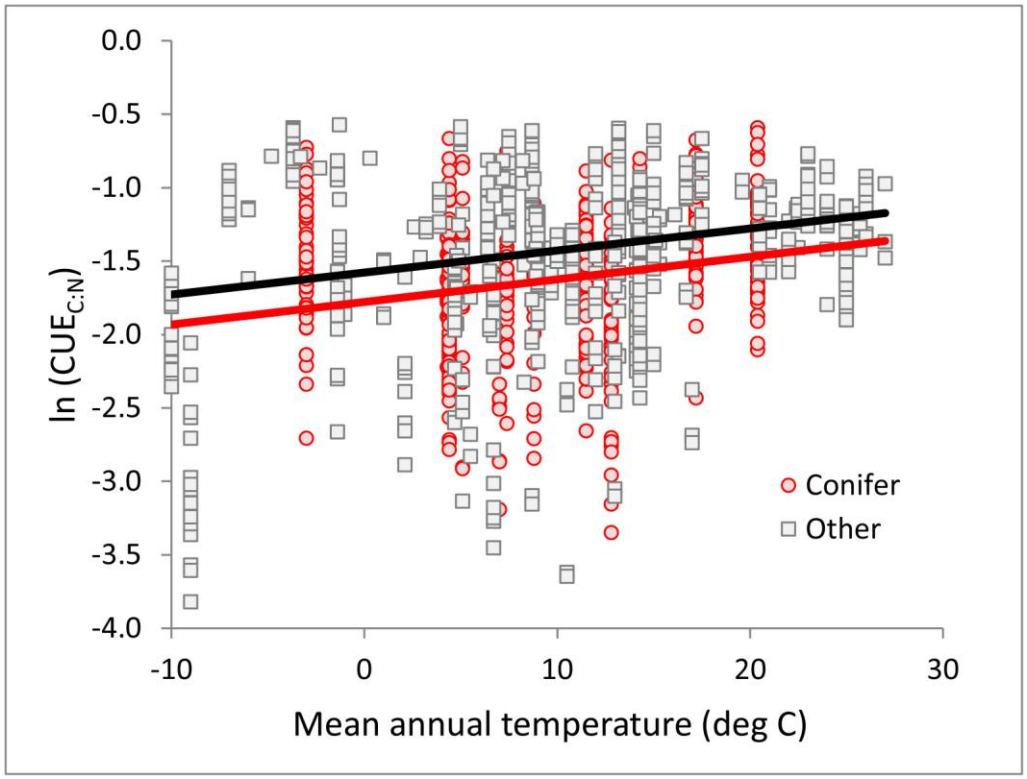

This article is protected by copyright. All rights reserved.

Accepted Article

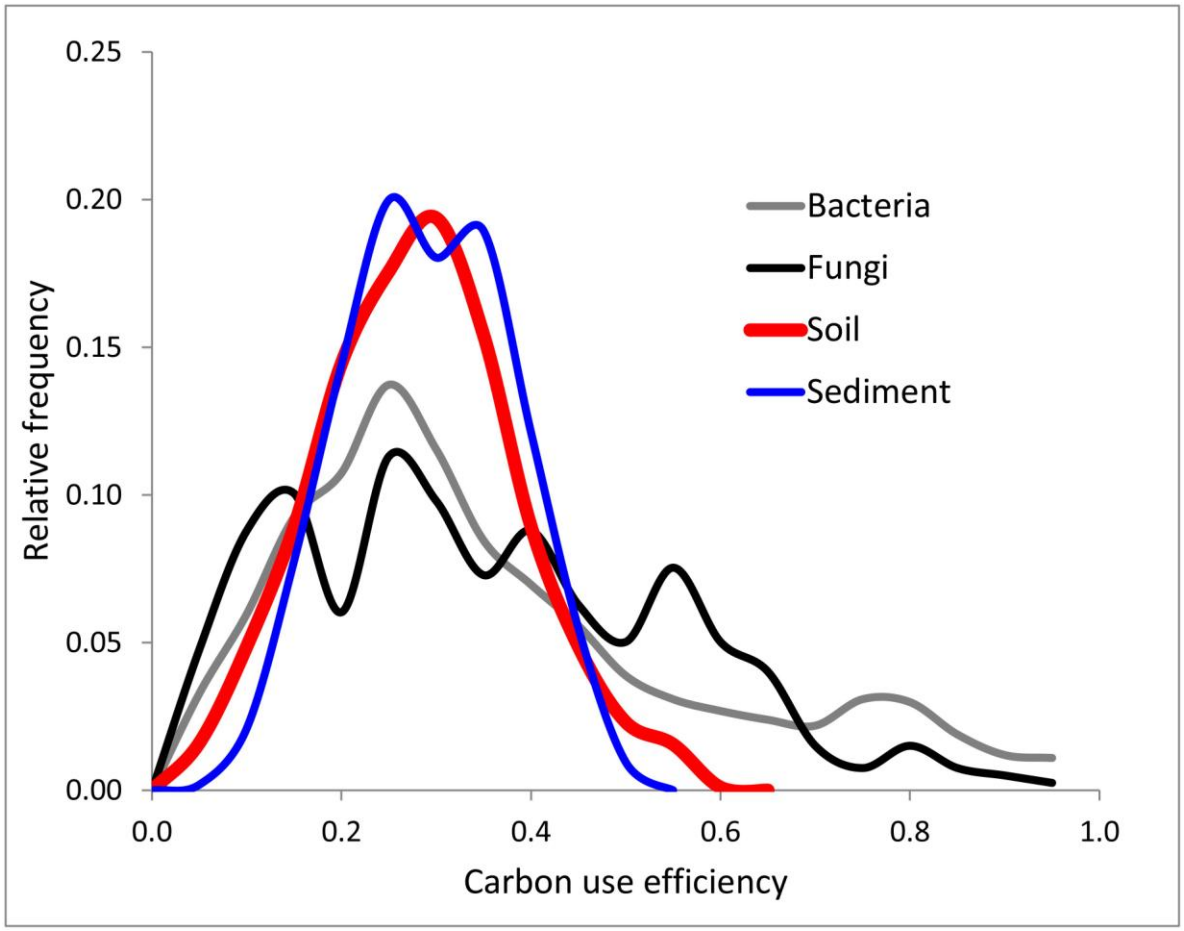

This article is protected by copyright. All rights reserved.